Journal of Loss Prevention in the Process Industries 43 (2016) 629–653

Contents lists available at ScienceDirect

Journal of Loss Prevention in the Process Industries

journal homepage: www.elsevier.com/locate/jlp

Quantitative risk analysis of loading and offloading liquefied natural gas (LNG) on a floating storage and regasification unit (FSRU)

M.R. Martins [a,*], M.A. Pestana [a], G.F.M. Souza [b], A.M. Schleder [a]

[a] Analysis, Evaluation and Risk Management Laboratory (LabRisco), Naval Architecture and Ocean Engineering Department, University of São Paulo, Av. Prof. Mello Moraes, 2231, 05508-030, São Paulo, Brazil

[b] Mechanical Engineering Department, University of São Paulo, Av. Prof. Mello Moraes, 2231, 05508-030, São Paulo, Brazil

ARTICLE INFO

Article history:
Received 14 January 2016
Received in revised form
1 August 2016
Accepted 1 August 2016
Available online 7 August 2016

Keywords:
Liquefied natural gas (LNG)
LNG offshore terminal
Quantitative risk analysis
Floating storage regasification unit (FSRU)
Preliminary hazard analysis (PHA)

ABSTRACT

Natural Gas is becoming an important energy source option and the capacity of the world to produce it is surging. Large reserves of natural gas exist worldwide, particularly in areas where the resources exceed the demand. Therefore, natural gas is liquefied for shipping; and its storage and regasification process usually occurs in onshore facilities. Recently, Liquefied Natural Gas (LNG) offshore terminals have been proposed as an attractive alternative solution. This paper presents a complete quantitative risk analysis (QRA) of undesired events that may occur during the loading and unloading of Liquefied Natural Gas (LNG) considering a typical LNG carrier and an offshore terminal similar to those operating in Brazil. Initially, a historical survey of accidents at LNG facilities, along with a detailed study of LNG carriers and LNG offshore terminals, is presented to support hazard identification. Once the potential hazardous events are categorized in some possible scenarios, a probabilistic potential hazard assessment is performed; moreover, the frequencies of occurrence of the undesired events are estimated. Afterwards, traditional consequence models are briefly discussed aiming to identify the weakness of each one that supports the specification of the model used in the consequence analysis of a specified case, which is evaluated by providing the data to estimate the total risk of the installation. The risk is evaluated in terms of social and individual risk. Lastly, possible control measures able to reduce the frequency of occurrence, or mitigate the impacts associated with the analyzed scenarios, are proposed and new risks levels are estimated by considering those control measures. The paper presents a complete QRA, presenting the tools and the models chosen to perform the analysis as well as some of the advantages and limitations regarding the use of these tools and models.

1. Introduction

The use of natural gas in the world is mainly conditioned to current energy demand peaks, which increase due to higher consumption generated by new technologies. Being a fuel virtually free of sulfur and ash, its combustion is very clean, thus offering a lower risk nature when compared to coal or mineral oil. In addition, gas plants are also flexible in technical and economical terms (Martins and Schleder, 2012).

In 2004, Brazilian natural gas demand was intensified due to the strong natural gas price reduction policy as compared with other energy sources – fuel oil, liquefied petroleum gas, gasoline and ethanol – thus encouraging the replacement of other energy source with the use of natural gas in different sectors. This policy was well accepted until 2004, when natural gas cost was well stabilized. However, in 2005, there was a reversal of policies in the national and international markets, and gas prices were slightly increased. At the time, Bolivia was the only international natural gas supplier for Brazil through the GASBOL pipeline. In May 2006, the Bolivian government threatened to cut off the gas supplies to Brazil, exposing the weakness of the Brazilian supply chain. Costs continued rising and, in 2008, there was a very significant increase. The imbalance in supply conditions and the demand for natural gas in Brazil, combined with the uncertainty regarding the supply of Bolivian gas, the country felt the need to adopt alternative suppliers in order to increase gas supplies and to ensure the continued provision of this energy source (ANP, 2010). In this context, LNG emerged as an additional source of natural gas, supplied by

* Corresponding author.
E-mail address: mrmartin@usp.br (M.R. Martins).

http://dx.doi.org/10.1016/j.jlp.2016.08.001

shipping transportation, but a specialized terminal was necessary to receive LNG carriers.

Within this scenario, a new option for the LNG storage and regasification arose, the Floating Storage and Regasification Unit (FSRU). The FSRU, which works as an offshore terminal, provides an economic and flexible option for the storage and regasification processes (Natacci et al., 2010; Schleder et al., 2011a). A FSRU costs less than an onshore facility of similar capacity and provides a faster return on the capital invested. It saves time by not demanding extensive planning and permits its process to occur with onshore developments, reducing construction time, assuming the conversion of an existing LNG carrier. Additionally, FSRU are flexible, since they can be moved from one demand area to another, which is an attractive feature in countries with seasonal demand, or where the market is unstable. It is also worth noting that an accident in one onshore plant might produce considerable impact on the neighboring areas and their population; this risk may be even worse due to the possibility of a terrorist attack (Martins and Schleder, 2012; Natacci et al., 2010; Ramos et al., 2011; Schleder et al., 2011b).

Aiming to guarantee the supply of natural gas for the internal demand, the first operating FSRU in the world was developed in Brazil. There are currently three LNG regasification offshore terminals in Brazil. One, known as Pecém, is located on the northeast coast, in the city of São Gonçalo do Amarante, in the state of Ceará. It has a LNG storage capacity of 129 000 m^3 (Blakwell and Skaar, 2009). Another terminal is located on the Guanabara Bay, on the coast of Rio de Janeiro, with a capacity of 138 000 m^3 (Blakwell and Skaar, 2009). In January 2014, a third terminal began to operate in Baía de Todos os Santos, Bahia, with a storage capacity of 175 000 m^3.

Ramos et al. (2011) and Ramos et al. (2014)compare the areas impacted by undesired events in onshore and offshore terminals in addition to possible consequences of LNG leakages. Essentially, an onshore terminal may generate smaller vulnerability distances compared to an offshore terminal, considering the same scenarios. However, in specific cases – such as the Brazilian terminals – an offshore would be more desirable due to the population near the coast.

This paper describes a comprehensive quantitative risk analysis for loading and unloading liquefied natural gas on ships, and proposes control options based on Liquefied Natural Gas Carrier, and a FSRU operating as an offshore terminal. In this context, it also addresses general topics, such as a description of natural gas and its transportation by ships, the reserves of LNG in the world, a historical survey of accidents involving LNG as well a case study of a typical installation very similar to offshore Brazilian terminals.

The risk analysis was conducted based on the Formal Safety Assessment (FSA) proposed by the International Maritime Organization (IMO, 2013). It started from defining the problem, followed by the identification of hazards, using the preliminary hazard analysis technique (PHA). Later, a risk analysis was conducted by investigating the frequency of occurrence and possible consequences of the identified potential hazardous scenarios; finally, effective and practical risk control options were proposed.

The consequence for the possible undesired events was evaluated using Phast Risk (DNV, 2009a,b), software developed by Det Norske Veritas and Germanischer Lloyd (DNVGL), and its frequencies of occurrence were determined based on the approach of the available databases.

2. Problem definition

The focus of this paper lies on the quantitative risk analysis of the LNG carrier for loading and offloading operations on a FSRU used as an offshore terminal considering the individual and the social risk as the measures of the risk. A typical LNG carrier and a FSRU similar to those operating on the Brazilian coast are considered. A practical methodology, FSA, was applied to explore the risks involved in a LNG Terminal and steps 1, 2 and 3 were applied. FSA is a structured and systematic methodology, aimed at enhancing maritime safety, by using a risk analysis and a cost benefit assessment (IMO, 2007). Fig. 1 shows the steps proposed by the FSA flow chart.

Applying step 1, a list of hazards and associated scenarios were identified and ranked according to their consequences and frequencies of occurrence, based on a qualitative risk analysis. In Step 2, a detailed quantitative investigation of causes and consequences of the most important scenarios identified was made. Finally, in step 3, risk control options (RCO) were proposed to reduce or to minimize the results from step 2. In addition, a future study on the costs and benefits can be applied, helping the recommendations to be taken by decision makers in an auditable and traceable manner, as suggested by the FSA in steps 4 and 5.

3. About LNG

This section will examine the physical and chemical characteristics of LNG, its production and logistics for storage and distribution around the world. The importance and the characteristics of carriers ships, receiving terminals and the possible risk of an accidental scenario during the loading and unloading (offloading) of LNG will be discussed, considering a FSRU as an offshore terminal.

Liquefied natural gas (LNG) is the cleanest burning fossil fuel, obtained from natural gas that has been cooled to -162 °C under atmospheric pressure, to become liquid. The composition of LNG is approximately 95% of methane, varying according to the source. Initially, to produce LNG, all impurities – such as water, heavier liquids, carbon dioxide, hydrogen sulfide – are removed to prevent freezing, which may cause blockages or damages to the equipment. Next, the gas is liquefied by a cooling process, shrinking its volume by 600 times, and turning it into a clear, colorless, odorless, noncorrosive and non-toxic liquid. The process to transform natural gas into LNG extracts the propane and butane from natural gas, which can be sold separately, or used as refrigerant in the cooling process. Therefore, the liquefaction of the gas allows for easier storage, along with economic and safe transportation by ship.

Briefly, the LNG value chain can be divided into the following stages: exploration, liquefaction, transportation, storage, regasification and distribution, as shown in Fig. 2.

Natural gas is plentiful in the majors proved reserves located in Middle East Europe and Eurasia, which share 73.7% of gas. Iran has the major proved reserves sharing 18.2%, followed by the Russian Federation and Quatar with 16.8% and 13.3%, respectively. The rank of proved reserves can be viewed in Annex A (British Petroleum, 2014).

The export and import of gas cases is very difficult because resources are usually in remote locations. Transporting the gas over long distances by pipeline becomes costly and impractical. In this case, liquefaction helps to transport the gas by ship, increasing safety, because liquefied gas is not flammable. Fig. 3 shows the trade flows worldwide (billion cubic meters) occurred in 2013 by pipeline, and by ship represented in red and blue arrows, respectively. In Brazil, these values are expected to increase due to future deployments of the Suape (PE) and Campo Grande (RS) terminals.

3.1. Transportation by ship

As previously mentioned, LNG carrier is the only economically viable alternative to gas transportation over long distances. As there were only a few incidents with no fatalities in the last 30 years, LNG carriers are considered safe; however, the occurrence of

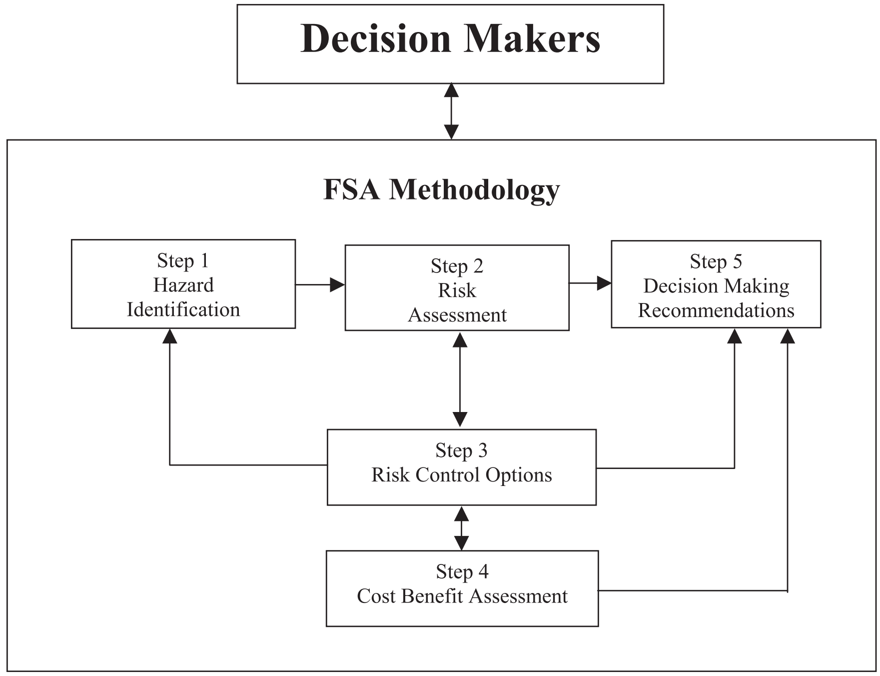

Fig. 1. Flow chart of the FSA methodology (IMO, 2007).

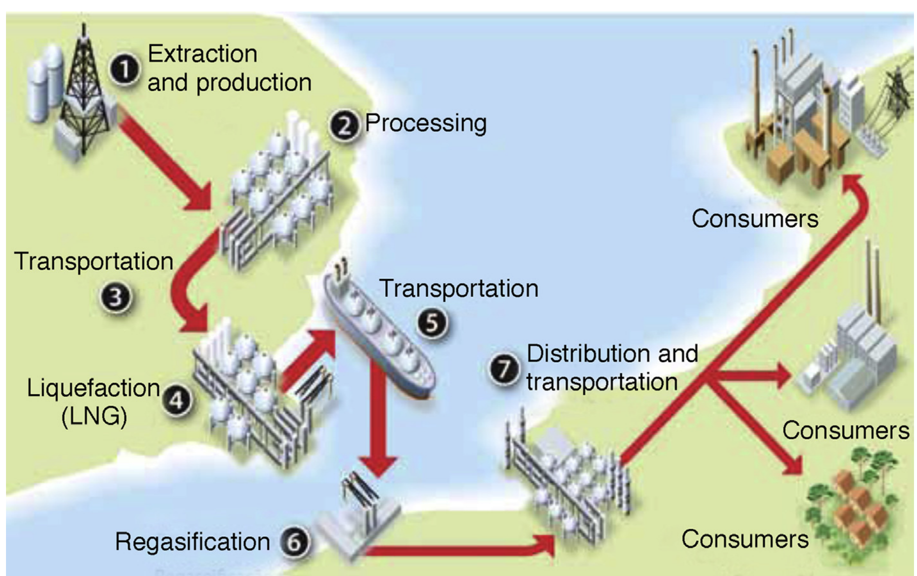

Fig. 2. LNG value chain (ANP, 2010).

an accident could lead to catastrophic consequences, considering the inherent cargo energy. Annex B addresses a survey on accidents involving plants handling LNG, in which none of the records available led to the occurrence of significant events during transportation. However, with the growing increase in new orders for ships with increasing load capacity and, therefore, larger vessels (draft, stranding risks), the risk factors tend to increase considerably. The application of international building code-based and special procedures for handling LNG reduces the risk of accidents on LNG carriers. This includes strict construction rules (double hull, double bottom), insulation of cryogenic load (special insulating materials), control systems, monitoring and mainly because of the specialized and trained crew. Fig. 4 shows some construction types of a containment system applied to LNG Carrier.

In membrane systems, thin stainless steel membranes, directly supported by the hull structure, contain the LNG. For the Moss system, the tank structural integrity is independent of the ship and spheres built from aluminum contain LNG. There are other types of self-supporting independent tank designs such as prismatic containment. A comparison of the safety and reliability of these systems is shown in Table 1.

3.2. LNG terminal

In most cases, LNG onshore terminals are responsible for receiving, storing and distributing LNG to costumers. When the terminal receives a LNG Carrier, the LNG is unloaded and usually stored before delivery to customers.

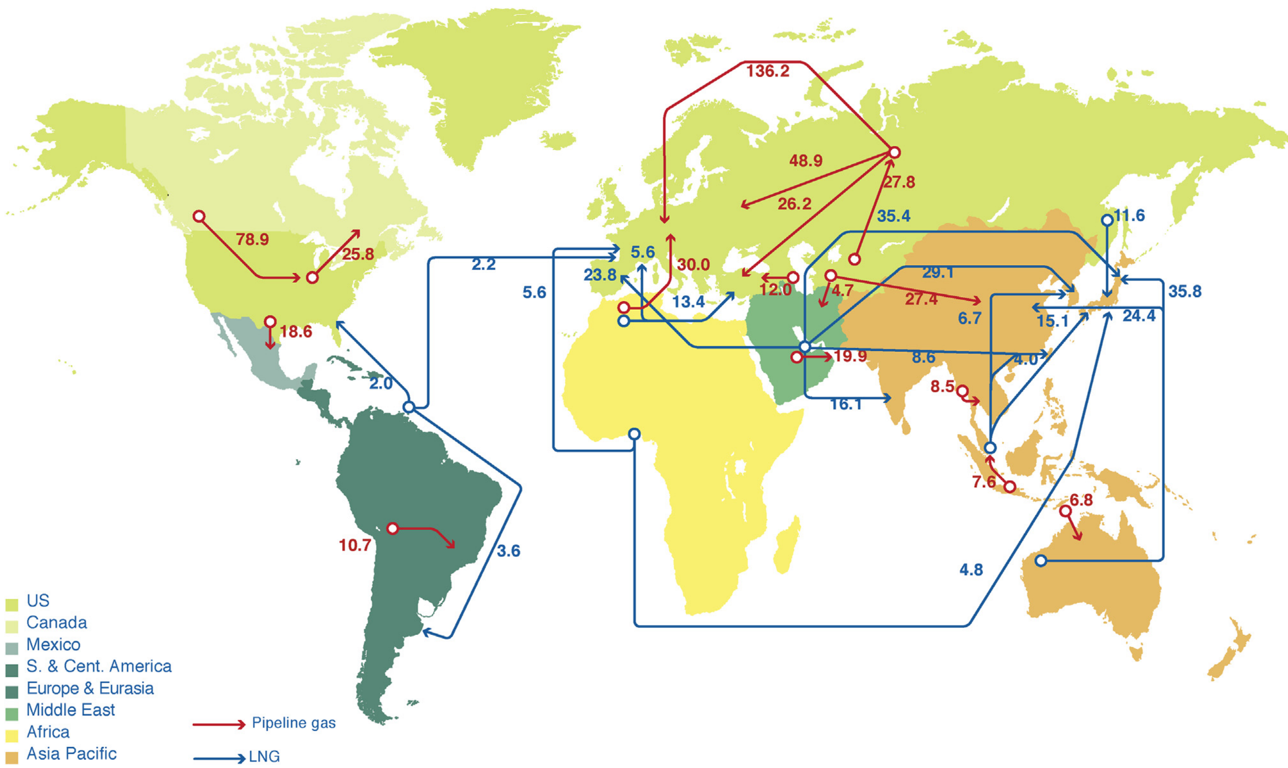

Fig. 3. Major trade movements in 2013 (Petrobras, 2015).

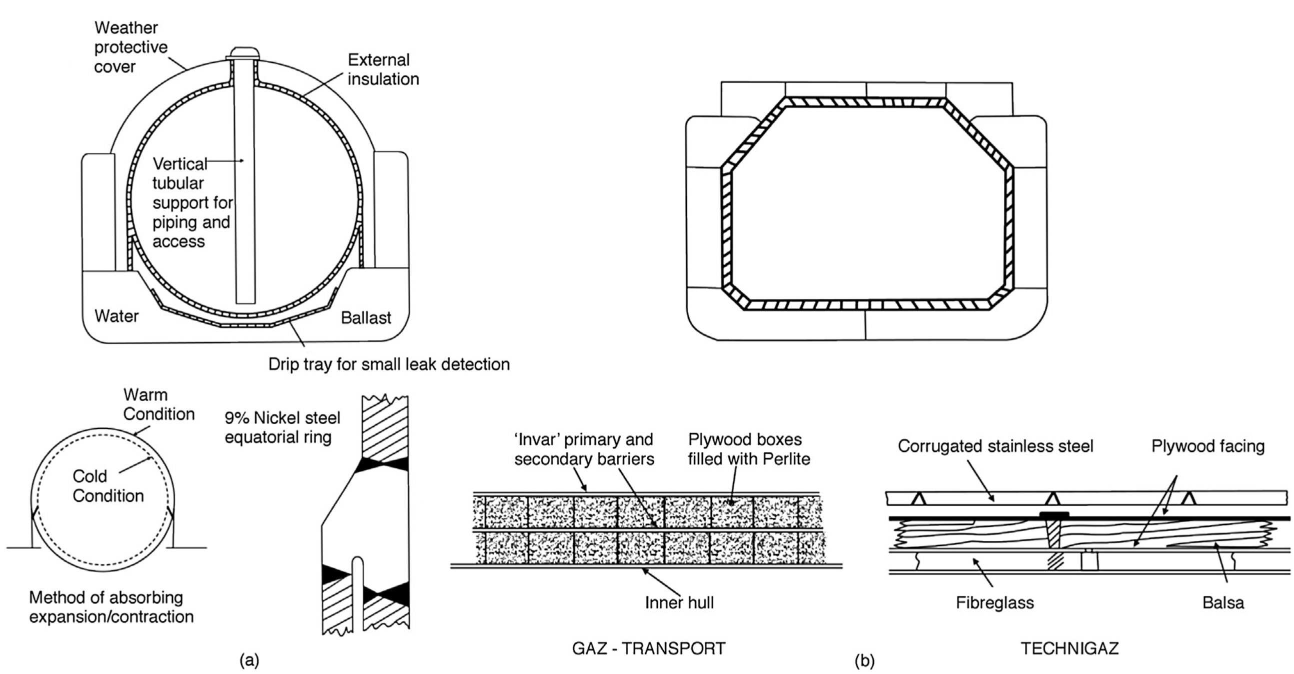

Fig. 4. Tank containment systems: (a) Kvaerner-Moss Spherical tank (b) Membrane Tank (at right) (Eyres and Bruce, 2012).

In the case of the FSRU used as an offshore terminal, as for the Brazilian case, the terminal has the same functions as an onshore terminal, but it has the advantage of being able to transport LNG to another location when required. This represents advantages in economic terms and contributes to the flexibility in the process of storage because a FSRU costs less than an onshore facility with the same storage capacity and reduces deployment time.

Loading and unloading operations in terminals involve many hazards because any leakage can generate major consequences for the local population and neighboring facilities (Martins et al., 2011, 2014; Natacci et al., 2010; Ramos et al., 2011). Under this perspective, a case study is conducted exemplifying the case of an FSRU loading and unloading LNG, which is very similar to Brazilian terminals. This terminal is 1950 m away from the coast and is capable of transferring a maximum of 10 000 m^3/h during loading and unloading operations (offloading). A minimum depth of 18 m was considered in the terminal area. An external berth to receive LNG carriers (LNG supply vessels) up to 315 m with two arms to offload

Table 1
Comparison of safety and reliability of different storage systems. Adapted from OTA (1977).

	Safety in event of vessel grounding/collision or other emergency	Reliability of containment system
Prismatic tank	Compared with membrane system, less likelihood of hull damage being transmitted to cargo tanks. More efficient use of cubic space.	Most ship year operating experience and most experience without primary barrier failure. Structure can be analyzed and the risk of fatigue failures minimized. Tanks can be constructed and 100% inspected prior to their installation in the vessel
Spherical tank	Safest system in event of grounding or collision – tank structure independent of hull and most void space between vessel hull and cargo tanks. Spherical tanks can be pressurized for emergency discharge in case of cargo pump failure.	Tank system easier to analyze structurally and therefore more reliable.
Membrane tank	Damage to hull of vessel may be more easily transmitted to the tank structure than with free-standing tanks. Membrane systems are also more reliable to damage or puncture due causes such as: a. Surging of cargo in tank b. Entering the tank for inspection or repair.	Structure cannot be analyzed easily making it difficult to assure the absence of fatigue failures. This could potentially lead to costly off-hire and repair time over the project life.

the LNG and one arm to return the LNG vapors (boil off) to the carrier. In addition, an internal berth prepared to receive FSRU up to 300 m with five transfer arms: two used to receive the LNG from the supply vessel; one used to return the LNG vapors to the carrier; and the other two to unload the regasified natural gas to the distribution piping. Fig. 5 shows a similar terminal considered the case study in this paper. The FSRU was considered with a total storage capacity of 130000 m^3, divided among 5 tanks, each with 26000 m^3, and equipped with an Emergency Shutdown System (ESD), controlling and monitoring the stages of offloading and interacting with an intercommunication process, (interlink) between the FSRU and the carrier, besides being designed to identify a failure in 30 s andto close ESD valves in 30 s.

In Brazil, the FSRU projects originate from the LNG Carrier implemented with regasification systems. Fig. 6 shows a sample of a schematic flowchart of a FSRU where two paths are presented: one where the LNG flows (represented by the blue bold lines) and the other where the boil-off flows (represented by the yellow lines). The blue lines are responsible for transferring LNG between carrier and platform, through manifolds connected to the cryogenic arms shown in Fig. 5.

During the transfer process, the LNG is vaporized – due to the heat exchange with the storage system – and should be redirected to the boil off line in order to prevent overpressure in the storage tank of the FSRU and pressure drop in the LNG storage tank carrier. In case of overpressures, undesirable scenarios may occur, such as gas release into the atmosphere, through the relief valves or the collapse of the structure. Low pressures can cause incoming atmospheric air into the tanks, heating and vaporizing the LNG. The boil off can also be used as energy source in the LNG carrier or the FSRU engine room as represented in Fig. 6.

Fig. 5. Brazilian LNG Terminal with transfer arms Petrobras (2015).

4. Quantitative risk analysis

This section presents the quantitative analysis of the potential risks in operations of loading and unloading LNG, evaluating possible potential risk scenarios. This includes LNG leaks caused by the failure of the components of FSRU during loading and unloading operations. Section 4.1 describes the performed hazard identification in order to determine the possible accident that can occur during loading and unloading LNG in an FSRU terminal and discusses about how these hazards were grouped in specific scenarios. The probability of occurrence of these scenarios is evaluated in section 4.2. Section 4.3 analyses the available model for the consequence analysis aiming the identification and discussion about their weaknesses and choose which one must be used to evaluate the potential consequences for the scenarios of interest while section 4.4presents the obtained results from the consequence analysis. Finally, section 4.5 describes how the risk calculation is performed and section 4.6 presents the obtained results for social and individual risks.

4.1. Hazard identification

The history of accidents involving LNG facilities is very important issue and it was considered in the risk analysis. Compared with refineries and petrochemical plants, the LNG industry has an excellent history in safety; however, accidents with fatalities have been recorded. One of the major accidents involving an onshore LNG plant occured in Cleveland East Ohio in 1994. The accident

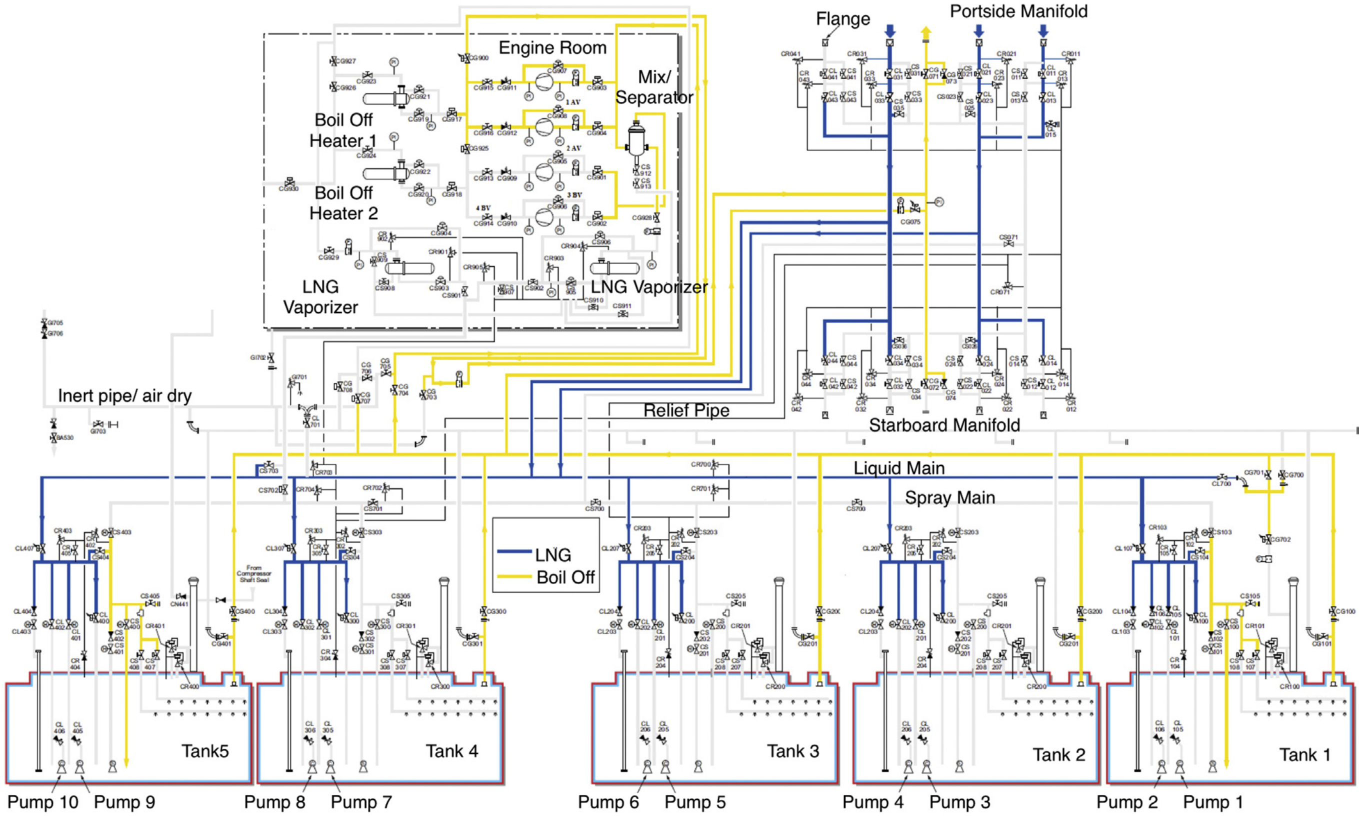

Fig. 6. Flowchart representation of FSRU Adapted from Martins and Souza (2011).

resulted in gas leak, explosion and fires, killing 130 people (CCNR, 2010; Ditali and Fiore, 2007; CH IV, 2015; Sovacool, 2008). There were other accidents involving fatal victims such as the cases in Staten Island in 1973 and Skikda in 2004 (ANP, 2010), which are listed in Annex B. In general, the major accidents did not involve maritime accidents. According to the U.S. Department of Energy, the LNG industry recorded some maritime accidents in the late 1960s resulting in fuel spillage and damage to the hull of the ship. Historical analysis indicates that accidents involving LNG in the world are rare, but their occurrence cannot be ignored, since there may be a chain of events, which can escalate to major accidents. IMO (2007) reported 182 events occurred in LNG carriers between 1964 and 2005. Some relevant events can be viewed in Annex C.

To set the system, its components, boundaries and functions is essential before starting the first step of FSA, hazard identification (HAZID). The system considered was discussed in section 3.2, which excluded from the analysis any component or system located outside the FSRU represented in Fig. 6. Furthermore, only the LNG loading and unloading operations were considered. Thus, all components and systems that have or may have direct contact with the LNG were included in the analysis.

By applying HAZID to this system, one hundred hazards were identified and explored through preliminary hazards analysis (PHA) technique. These hazards were identified according with the type of leakage, related causes, consequences and safeguard actions. Table 2 partially shows some of the hazards identified. The table is fully presented by Martins and Souza (2011).

All identified hazards were grouped according with the leakage characteristics and were classified into four scenarios, which were analyzed for the case study: small LNG leaks, medium LNG leaks, large LNG leaks due to catastrophic tank rupture and large LNG leaks due to line rupture. To classify the identified events, some considerations and assumptions were made regarding the leakages. For instance, events derived from the loss of sealing were simulated as being equivalent to holes with corresponding diameters of up to 100 mm; thus, they were classified as small leaks. It was considered medium leaks those resulting from the occurrence of holes with the equivalent diameters ranging from 100 to 200 mm. Finally, events of greater magnitude, associated with diameters greater than 200 mm, were considered catastrophic ruptures of the storage tank or pipe.

4.2. Probabilistic potential hazards assessment

In order to assess the risk involved in FSRU operations, it is necessary to evaluate the probabilities of the occurrence of identified hazardous events, which may be estimated from the historical frequency of potential events. However, for LNG spill events, frequencies, when available, present great uncertainties, making the development of studies related to the area difficult.

The Reference Manual Bevi Risk Assessments (RIVM, 2009) and Handbook Failure Frequencies (Flemish Government, 2009) defines default failure frequencies for equipment systems; however, they omit the number of flanges, valves and instruments associated with major equipment items. In order to fill this gap, the Health and Safety Executive (HSE), compiled the Hydrocarbon Release Database (HCRD), which is the largest database, containing information of over 4000 leakages events in oil and gas installations in the continental shelf of the UK, including data since 1992 (DNV, 2013; HSE, 2015). Thus, 78 different types and size categories of process equipment were identified and compiled. Moreover, the consideration of the number of flanges, valves and instruments associated justify the greater values proposed for the probability of leakage events occurrence when compared with the values proposed by other databases. The HCRD database is used in Leak software developed by DNVGL to estimate equipment leakage frequencies and to calculate the total leakage frequency of the installation (DNV, 2013) based on its specifications. The statistical value of the data allows its use in LNG facilities where there is a lack of data

Table 2
Part of the table developed in the PHA.

System: Loading and unloading system of the LNG carrier			
Hazard	Causes	Consequence	Safeguard actions
Large LNG leakage	Line rupture to bypass LNG to tanks 2 and 3.	Damage to the ship structure. Possible gas cloud formation. Freezing of the surrounding areas of the installation. Possible entrance of atmospheric air into the system, contaminating the inert environment. Interruptions of the LNG transfer process.	Existence of an emergency shutdown system responsible for stopping the process of loading/unloading in the event of a major leak. Existence of a monitoring system indicating the pressure and temperature of LNG. Existence of an alarm and control system responsible for detecting LNG leak and interrupting the transfer process.
Small LNG Leakage	Improper connection of at least one of the two cryogenic arms that transfer LNG through the manifold	Damage to ship structure. Interruptions of the LNG transfer process. Actuation of the emergency systems.	Installation of a containment basin at the bottom of the cryogenic arm connections to retain any possible LNG leakage after disconnection. Existence of a monitoring system indicating the pressure and temperature of LNG. Existence of an alarm and control system responsible for detecting LNG leak and interrupting the transfer.
Small LNG Leakage	Loss of structural integrity of the valves responsible for isolating the manifold	Damage to ship structure. Interruptions of the LNG transfer process. Actuation of the emergency systems.	Existence of an alarm and control system responsible for detecting LNG leak and for interrupting the transfer.
Large LNG leakage	Rupture of the storage tank	Damage to ship structure. Possible gas cloud formation. Freezing of the surrounding areas of the installation. Possible entrance of atmospheric air into the system, contaminating the inert environment. Interruptions of the LNG transfer process.	Existence of an emergency shutdown system responsible for stopping the process of loading/unloading in the event of a major leak. Existence of a monitoring system indicating the pressure and temperature of LNG. Existence of an alarm and a control system responsible for detecting LNG leak and interrupting the LNG transfer. Existence of a secondary tank capable of storing the LNG leaked from the damaged tank.

regarding cryogenic facilities for equivalence in LNG plants. In addition, the HCRD base enables to disregard the flanged connections, since the equipment and items that are not in contact with cryogenic materials present welded type connections.

Consequently, estimates of leakage frequencies in a FSRU were conducted by using the HCRD database (HSE, 2015) with Leak software (DNV, 2009a). From the FSRU described in section 3.2, it was possible to calculate the total leakage frequency considering the contribution for each FSRU component. Annex D and E present the list of components with the necessary information to estimate the expected frequency of the analyzed categories of leakage during loading and offloading, considering a FSRU similar to those operating on the Brazilian coast. Importantly, there are still no cases of events of catastrophic ruptures LNG storage tanks. This fact is justified by the high construction standards presented in section 3.1, which reduce the possibility of unwanted leaks. Thus, the estimation of catastrophic tank rupture frequencies was obtained by considering the value of the largest equipment and hole available in DNV in 0. Although the frequency of the proposed value tends to be different from the real value, a very conservative analysis is performed, since the frequency of events of this magnitude is rare. The software results for frequencies leak are shown in Table 3. Note that this value is the sum of the frequency of the valves, length of pipes and other components involved.

4.3. Performing the consequence analysis

When a flammable liquid is released from a storage tank or pipeline, the leaked substance may form a pool. Some of the liquid will evaporate and disperse; if the flammable cloud of vapor finds an ignition source, while concentrated between the lower and upper flammability limits (LFL and UFL), a flash fire and/or an explosion will occur, and, in this case, the flame can travel back to the spill causing a pool fire (Pitblado et al., 2006). A pool fire involves burning the vapor above the liquid pool as it evaporates and mixes with the air. This sequence is illustrated in Fig. 7. In case of a flash fire, the potential to injure individuals is restricted within the ignited gas cloud; however, the explosion can generate over pressure waves, outside the cloud limits. The potential for fatalities in pool fire is due to the exposure to heat radiation.

As previously mentioned, LNG is composed mostly of methane and it is a cryogenic liquid at −162 °C. Its lowest flammability level (LFL) is of 4.4% by volume and its high flammability level (HFL) is of 16.5% by volume. Therefore, a mixture with air within this range of concentration is flammable. The extremely low temperature of LNG and the potential for vapors to ignite in the presence of a spark are the key risks to be managed.

When LNG mixes with water or is exposed to a warmer surface, it initially forms a white and dense vapor cloud due to the condensation of the water present in the air. As the cloud is warmed by the heat received from the air and the substrates (water or ground), it becomes lighter than the air and dissipates as a passive cloud, leaving no lasting residue.

LNG vapors may burn when released to the atmosphere, but they do not release energy quickly enough to create overpressures, or forces, associated with explosions. The LNG ignited will cause a flash fire; then, it will flash back to the source, where the LNG spill can burn as a pool fire.

Generally, to obtain a more conservative analysis of the region subjected to the effects of the flash fire, the burning of the cloud is considered to occur when the maximum ground level footprint area is taken to the LFL Fraction (Moonis et al., 2010). Furthermore, the effects of pool fire are calculated based on the immediate and delayed ignition of the pool. It was considered an early pool fire when the fire begins at the releasing, while a late pool fire occurs when the liquid pool spreading is assumed to have taken place prior to ignition.

To evaluate the possible consequences of the potential hazardous events identified in the PHA, it was developed study of the models available in the literature and of the commercial software for consequence analysis. There are several types of models available that can be used for LNG modeling. Gaussian models are

Table 3
Event frequency.

Hole size	Total frequency (per year)		
	Loading circuit (Liquid leakage)	Offloading circuit (Liquid leakage)	Boil-off circuit (Gas leakage)
Small leaks (0–100 mm)	9.082×10^{-02}	9.535×10^{-02}	1.432×10^{-01}
Medium leaks (100–200 mm)	1.490×10^{-03}	1.485×10^{-03}	1.475×10^{-03}
Large leaks due line rupture (>200 mm)	6.785×10^{-03}	6.824×10^{-03}	7.321×10^{-03}
Large leaks due catastrophic tank rupture	8.537×10^{-04}		

influenced by atmospheric turbulence and ignore dense gas effects (Woodward and Pitblado, 2010). For this reason, they are not considered appropriate for dense gas dispersion consequences. The Slab model is appropriate to analyze the cloud dispersion resulted from dense gas releases; however, this model does not consider the effect of the crosswind during the release. The UDM model is a complete solution since it can evaluate any cloud dispersion (dense or buoyant) and it works with weather parameters such as wind velocity, atmospheric pressure, and temperature. However, as the Slab model, the UDM model do not consider the geometry of the dispersion field and the results can be compromised if the cloud dispersion occurs in an ambient presenting a complex geometry, confinement or barriers. Computer Fluid Dynamic (CFD) models use the fundamental equations of fluid flow (Navier Stokes equations) and are able to deal with complex and confined geometries; however, the cost of computational implementation greatly increases due to performing the calculations for complex models, such as models that have turbulence (Schleder and Martins, 2013). The GASP model describes the dispersion and the evaporation of the pool to estimate the evaporation rate and the size of the pool. Differently from GASP, the PVAP model assumes a minimum thickness of the pool, thus limiting pool dispersion. It also allows simulating the dispersion of the pool regardless of the boiling temperature of the liquid, initially considering the release and pool at the same temperature. Jet fire models can describe the shape of the flame by using the cone model or the API RP521 which treats the flame as a banana shaped plume (API, 1969; Baron, 1954; Cook and Woodward, 1993). The cone model treats the flame as a tilted cone frustum with three options of correlations. The correlation Johnson is appropriate for a horizontal vapor release (Johnson et al., 1994; Oke, 2005; TNO, 2005a,b). When a release is comprised of liquid or two-phases, the model correlation Cook (Cook et al., 1990) is more suitable (DNV, 2009a,b). For non-horizontal vapor release the correlation Chamberlain (Chamberlain, 1987) is recommended. As well as dispersion can, jet fires can be modeled by CFD tools. The use of the API RP521 model was preferred for this study due to the possibility of more conservative results. In order to check and compare the jet fire results from the API RP521 model a simulation using a CFD software (FLACS from GexCon (2013)) was also performed. A review of the software models made by Pitblado et al. (2006) considers that the Phast Risk (DNV, 2009a,b) is one of the best-validated consequence codes. This software applies the Unified Dispersion Model (UDM) to describe cloud dispersion, which incorporates the Pool Vaporization Model (PVAP) to evaluate the pool formation, its dispersion and vaporization. The program has two methods for calculating the effects of jet fires: The cone method based on Chamberlain (1987), JFSH-Johnson (Johnson et al., 1994; Oke, 2005; TNO, 2005a,b) or JFSH-Cook (Cook et al., 1990) correlations and the API RP521 model (API, 1969; Baron, 1954; Cook et al., 1990). Based on the importance of a wide validation of results from the code used in a quantitative risk analysis, the consequences analysis were conducted with the Phast Risk software, which includes the models previously discussed. Annex F summarizes the most used models in a consequence analysis presenting a brief description and the major references of each model.

4.4. Consequences results

Considering the input data presented in Table 4, the possible consequences of the scenarios, specified based on the results of the PHA were evaluated – small leak; medium leak; large leak due to line rupture; and large leak due to catastrophic tank rupture. Pump head is the equivalent head level for the energy added to the system by a pump. This value was considered to ensure the flow of 10.000 m^3/h. Based on the pump head, the leaked volume was calculated for small, medium and large leaks, due to line rupture, considering 30 s to detect leak and another 30 s to shut down the valves. For the large leak due to line rupture, medium l and small leak, the volume is 166.7 m^3, 69.2 m^3 and 17.25 m^3 respectively.

Weather conditions were considered based on the meteorological data on the Brazilian northeast coast (ANP, 2007), and reproduced in Table 5; whereas for atmospheric pressure, wind speed and humidity there is no differentiation between day and night.

In order to assure that the quantitative consequence analysis has been conservative, leaks were assumed to occur in the horizontal direction, except for those related to the instantaneous release of the inventory (i. e., large leak modeled as a catastrophic rupture). Simulations have been made considering different leakage directions, such as vertical downward, vertical upward, and angled to a horizontal line. The maximum areas subjected to possible impacts of cloud dispersions and thermal radiation emissions were observed to occur in case of leakage in the horizontal direction.

For each specified scenario, results were obtained for pool formation, its dispersion and evaporation; cloud dispersion; flash fire; pool fire; and jet fire. As examples, Figs. 8–11 illustrate the catastrophic tank rupture scenario; the pool radius as function of time, for both day and night weather conditions; the greater footprint of the cloud with its frontier concentration equal to 50% of methane LFL; the envelope of the flash fire event, which identifies the area subjected to a flash fire impact; and the radiation level as a function of distance to the leakage point, in case of occurrence of a late pool fire. Although the cloud does not burn at concentrations lower than LFL, it is conservatively recommended to consider the 50% of the LFL concentration to define a safe distance.

Fig. 8 shows that the pool radius is not dependent on the weather conditions since the lines for both conditions analyzed, night (black) and day (red), are almost overlapped. The program divides a release into segments, in order to reflect significant changes in the nature of the release over the course of the dispersion, such as changes in the vapor release rate. Thus, each horizontal dashed line represents the average radius calculated for each segment defined by the software. It is important to emphasize that the values of the average radius of the pool are needed for simulating the dispersion cloud after the use of dispersion segments. The PVAP model divides the dispersion into segments with constant evaporation rates (Cook and Woodward, 1993). The segments that correspond to the higher rates are therefore associated to the lower level of duration times. The results presented to the maximum pool radius in Fig. 8 are consistent with the amount of LNG released in catastrophic tank rupture scenario (26 000 m^3)

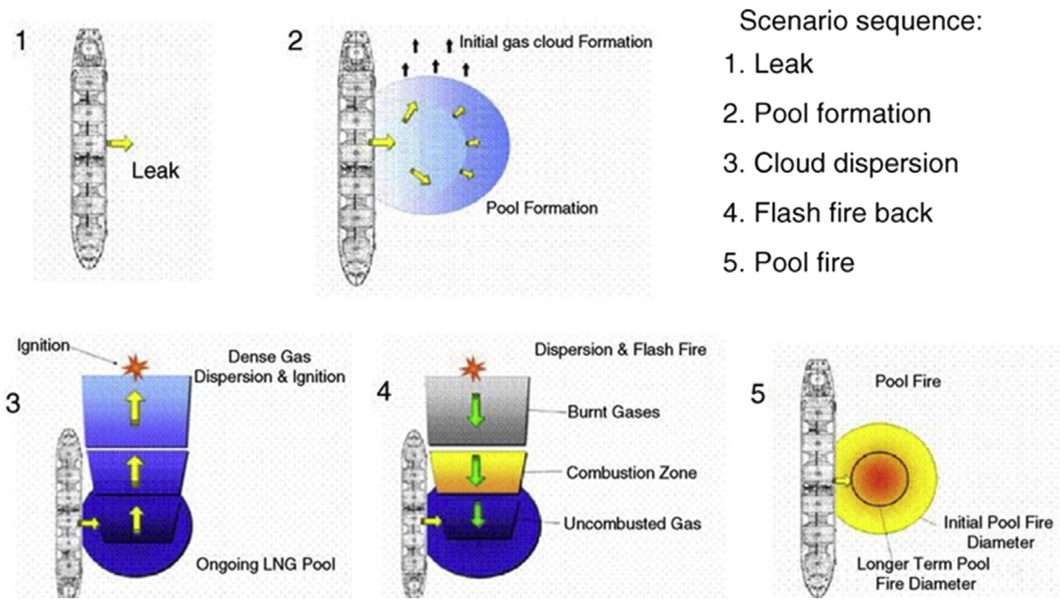

Fig. 7. Sequence of flammable release (Pitblado et al., 2006).

which occurs instantaneously without any containment barriers. Additionally, it is worthwhile to note that PVAP model assumes the undiked pool grows concentrically until reaches a minimum thickness (for water surfaces, 0,001 m). Thus the maximum pool radius of 500 m obtained is the result of low roughness of the contact surface – that is water – and release scenario.

Fig. 9 shows the greater cloud footprint at the instant at which its edges reach the concentration of 50% of the LFL for a catastrophic tank rupture scenario, considering day and night weather conditions. This figure shows that the maximum distances from the leakage point, possibly impacted by a flash fire occurrence, are 2690.84 m and 3621.81 m for day and night weather conditions, respectively. These distances, combined with the frequency of the event, can be used to define 'safe areas' according to the risk criteria established by the regulatory standards as P4.261 used in Brazil (CETESB, 2011). It is noteworthy that the night condition has a greater range due to more stable winds and atmospheric conditions. This stability reduces the air entrainment in the cloud and, consequently, its dilution is slower.

Fig. 10 shows the flash fire envelope identifying the area subjected to the consequences of a possible undesired event of flash fire. It is important to emphasize that, although the considerations related to the dispersion of the cloud were made for a specific direction (downwind), for the flash fire envelope graph, every direction is considered as being equally likely for the wind to blow. Thus, the maximum distance is assigned to all directions, resulting in an envelope of a circular shape, as presented in Fig. 10.

The solid and dashed red curves specify the flash fire envelope for day weather conditions, at ground level, when its concentration reaches the LFL and 50% of this value, respectively. The solid and dashed black curves show the same results for night weather conditions. Despite the impossibility of burning a cloud in concentrations lower than the LFL, the use of distances corresponding to 50% of this value is conservatively recommended.

Table 5
Weather conditions.

Atmospheric pressure	101.325 kPa
Wind speed	10.56 m/s
Average temperature	26.75 °C
Relative humidity	78%
Pasquill stability classes	Day: Stability class C Slightly unstable conditions Night: Stability class D Neutral Conditions

Fig. 11 shows the radiation level emitted by a late pool fire for a catastrophic tank rupture scenario as a function of the distance downwind and shows the radiation. As described in the next section, regarding the vulnerability for the occurrence of pool fires, fireballs and jet fires, CETESB (2011) recommends adopting the fatality probability equal to 100% (1.0), when the heat radiation is greater than or equal to 35.0 kW/m^2 and of 1%, when the heat radiation is 12.5 kW/m^2. The exposure time to be used is of 20 s, except for fireball, which should use its duration, up to the 20 s. Note that for the distance of approximately 500 m, the radiation remains constant because this value represents the diameter of the pool.

Finally, Fig. 12 shows the radiation level emitted by the jet fire for a small leak scenario as a function of the distance downwind. Note that the maximum flame radiation, about 254,39 kW/m^2, falls rapidly after approximately 153 m. This thermal heat flux can damage process equipment and cause the collapse of mechanical structures (Jang et al., 2015). Since the results concerning to jet fire consequences were so critical, the same scenario was evaluated by using a CFD software FLACS (GexCon, 2013) to check and compare

Table 4
Input parameters used in phast risk.

Scenario type	Leak (small)	Leak (medium)	Line rupture (Large)	Catastrophic tank rupture (Large)
Material and conditions	Methane (CAS Id 74828) at −162 °C and at Atmospheric Pressure			
Volume	17.25 m^3	69.2 m^3	166.7 m^3	26 000.00 m^3
Pump head	189.3 m	189.3 m	189.3 m	N/A
Pipe internal diameter	N/A	N/A	310.8 mm	N/A
Equivalent hole diameter	100 mm	200 mm	N/A	N/A

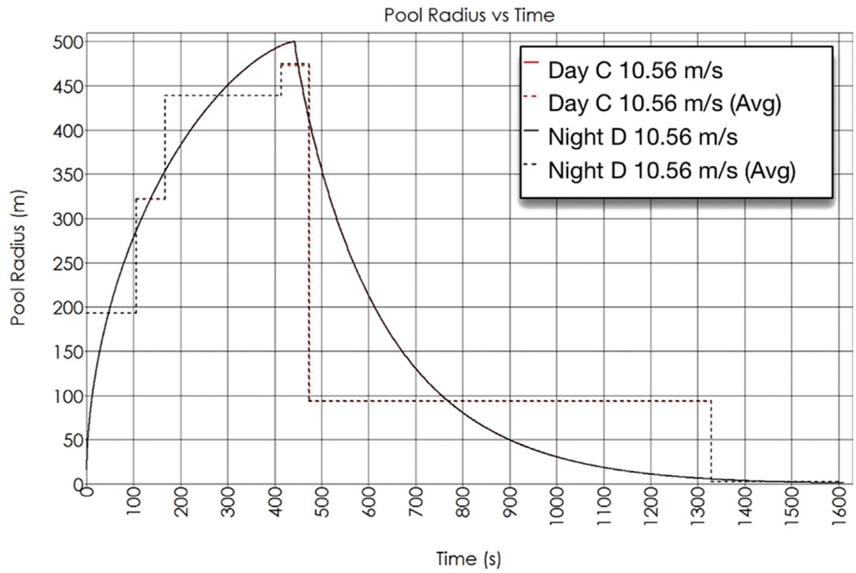

Fig. 8. Pool radius as a function of time for both day and night conditions for the catastrophic tank rupture scenario.

the results. The safe distance defined by the results from CFD model is slightly more critical; the values from CFD model are represented by the red dots in the chart and the distance associated to the 35 kW/m^2 radiation level was 190 m. Concerning flame length, since the jet is horizontal and dense, the flame length was estimated from the position where the fire touches the ground, which in this case was about 140 m from the release point; however, fire continues to spread over the surface after this point. It is worth to note that the CFD simulation was evaluated assuming the same hypotheses present in the API RP521 model and a less conservative approach could generate different results.

From the analysis of the graphs and with the aid of the reports generated by the software, the results were evaluated concluding the quantitative consequence analysis. The results summarized for small, medium and large leaks are presented in Table 6. Note that for large leaks due to catastrophic tank rupture, no result is generated for jet fires due to its instantaneous release. Further information can be found in Martins and Souza (2013), where the consequence analysis is fully detailed.

4.5. Performing risk calculations

Risk is the measure of harm to human life, property, or environmental damage, resulting from the combination of the frequency of occurrence of one or more accident scenarios and the magnitude of the physical effects associated with these scenarios. As determined in the problem definition, the risk analysis performed used the individual risk and the social risk as the risk measure.

The risk values obtained were interpreted based on the CETESB standard P4.261 (CETESB, 2011) – Risk of accident of technological origin – method for decision-making and reference terms. CETESB is the State of São Paulo Environmental Company and the P4.261 standard establishes guidelines for estimating the risk and specifying the tolerability criteria, which must be used by the official governmental agency to decide on the viability of any industrial installation concerning its risk aspects.

Individual Risk is the risk experienced by a single individual in a given time period, meaning the probability of a fatality or an injury of someone located in the surrounding areas. The individual risk considers that the person is at a specified location and is expressed through the Risk Contour Plot. For individual risk assessment, P4.621 standard 0 suggests the risk classification into three different levels, as shown in Table 7.

The not tolerable level indicates that the risk cannot be justified and the implementation of mitigation and contingency measures are mandatory. ALARP stands for the "as low as reasonably practicable" level and considers the risk is tolerable, but the implementation of all possible measures is suggested to prevent the risk exceeding the limit of 10^{-6} per year. Finally, tolerable level suggests

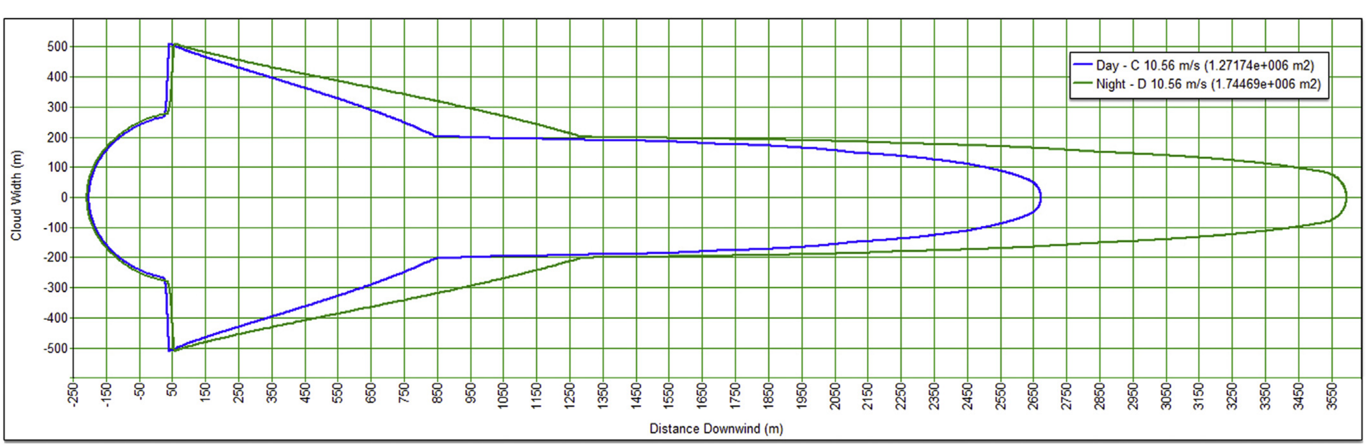

Fig. 9. Greater footprint of the cloud with its frontier concentration equal to 50% of the methane LFL for the catastrophic tank rupture scenario.

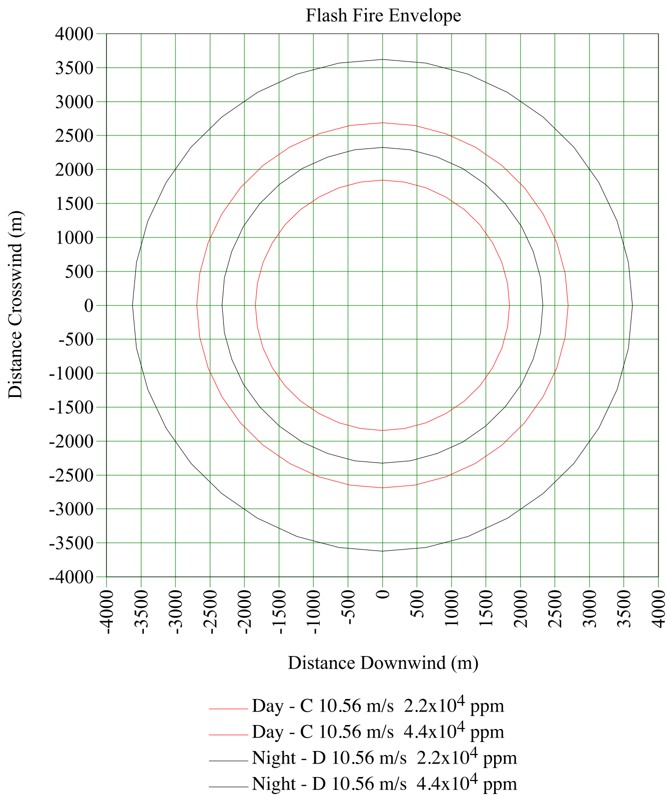

Fig. 10. Area subjected to a flash fire for the catastrophic tank rupture scenario.

that no action is required to reduce the risk.

Social risk is the probability of a certain group of people, located near the hazard area, to suffer some specific type of injury or fatality due to exposure time and the result of the accidental event in question. Its expression is given by means of FN curves, where F is the cumulative frequency of occurrence of the potential hazardous scenarios, with N or more fatalities. To evaluate the social risk, P4.621 standard suggests the criterion shown in Fig. 13, where the limits are applicable only to extramural individuals. Thus, similarly to the individual risk criteria, it does not include people that are in the facility.

The area located above the upper limit (represented by the solid red line) is considered a not tolerable risk. The area under the lower limit (represented by the green dashed line) is considered a tolerable risk. The intermediate region between the dashed green and solid red lines is considered areas where the risk must be reduced as much as possible through mitigation measures or project reassessment.

To evaluate social and individual risk, the evolution of each identified potential hazardous scenarios analyzed using the event tree technique should first be known. The next section discusses the event trees considered to estimate the individual risk close to the FSRU.

4.5.1. Event tree scenarios

A given release or event may develop in different ways; and each path has its own probability and its own set of hazardous effects. For example, a release may ignite immediately or after some delay; the immediate ignition may result in an explosion, a flash fire, or a fireball, while a late ignition may result only in a flash fire.

The event tree considered to estimate the individual risk close to the FSRU is related to the catastrophic tank rupture, as the initiating event is shown in Fig. 14. This event tree identifies the possible hazardous scenarios in a specific location close to the FSRU. The output frequency is the probability of an event occurrence in one year. The individual risk in point is the result of an accidental frequency of scenario combined with the likelihood of wind occurrence toward the point, i.e., 25% due the simplification of wind direction probabilities into 4 equal directions. This consideration was assumed in order to contribute to the calculation of the individual risk, since it simplifies the results of the event tree.

For stationary installations such as a FSRU Terminal, the probability of occurrence of an immediate ignition is estimated according to the substance category and the output flow, as suggested in RIVM (2009). Table 8 presents the recommendation for the immediate ignition probabilities values according to the output flow and substance category.

The definition of the substance category is given in Table 9, which is the WMS category (Wet Milieugevaarlijke stoffen), a classification and labeling of chemicals for Environmentally Hazardous Substances (EHSNR, 2015). The reactivity of a substance is its susceptibility to flame acceleration, determined based on the size of the explosion area, minimum ignition area, spontaneous

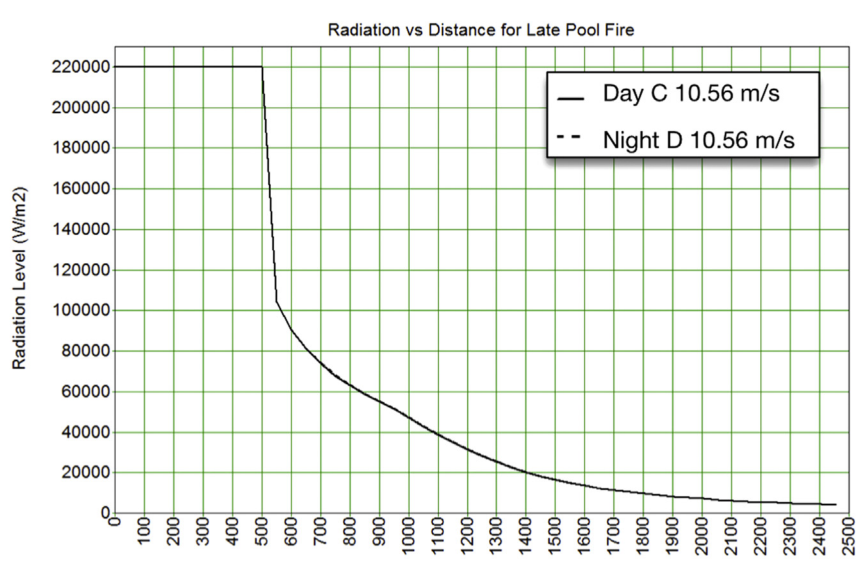

Fig. 11. Radiation vs Distance for Late Pool Fire for the catastrophic tank rupture scenario.

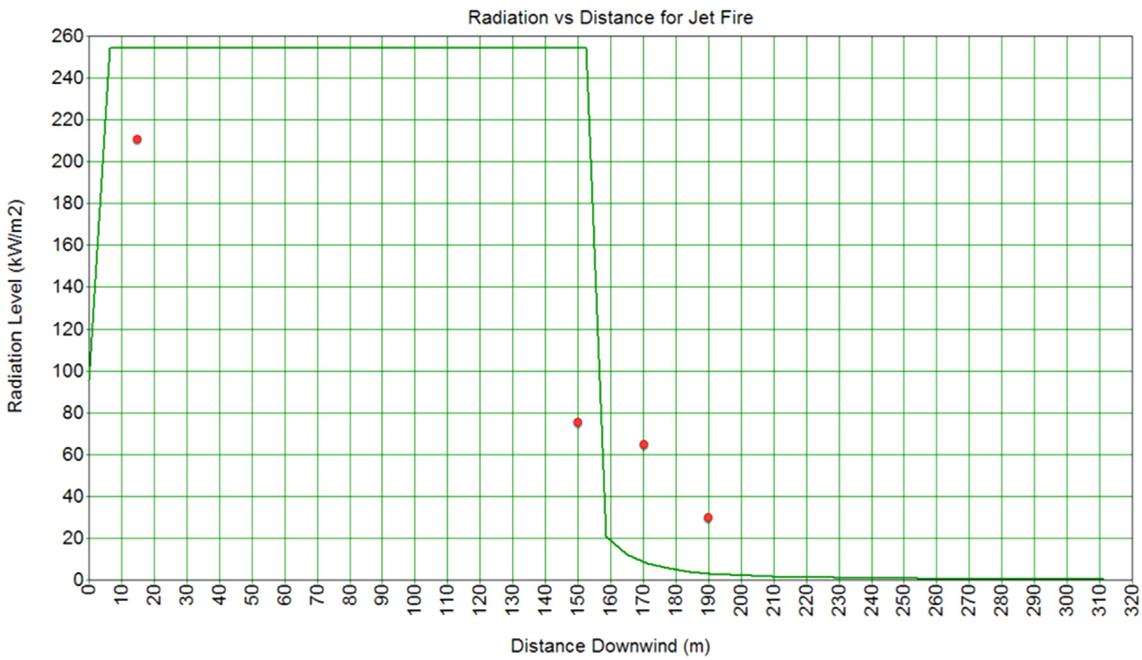

Fig. 12. Radiation vs Distance for Jet Fire for the small leak scenario.

Table 6
Summary of results for the simulation of the scenarios considered.

	Small leak		Medium leak		Large leak due to line rupture		Large leak due to catastrophic tank rupture	
	Day	Night	Day	Night	Day	Night	Day	Night
Pool formation, dispersion and evaporation								
Maximum radius of the pool	18.50 m	18.40 m	37.85 m	37.90 m	57.30 m	57.32 m	499.58 m	500.10 m
Mass released to the pool	5975.15 kg	5910.24 kg	26 588.07 kg	26 690.37 kg	67 835.07 kg	67 750.07 kg	10 820 814.11 kg	10 833 519.84 kg
Mass vaporized from the pool (60s after the beginning of the pool)	3657.70 kg	3620.99 kg	10 906.68 kg	10 959.74 kg	19 485.23 kg	19 470.06 kg	501 266.20 kg	496 067.78 kg
Remaining mass in the pool (60s after the beginning of the pool)	2317.45 kg	2289.25 kg	15 681.38 kg	15 739.63 kg	48 349.84 kg	48 380.01 kg	10 319 547.91 kg	10 337 452.06 kg
Cloud dispersion								
Distance for the first contact between cloud and water	4.92 m	4.92 m	4.22 m	4.20 m	1.78 m	1.90 m	1.84 m	2.41 m
Distance to *rainout*	12.19 m	13.25 m	13.94 m	13.17 m	7.82 m	8.31 m	2.34 m	3.05 m
Maximum distance reached by the cloud for a concentration of 50% LFL in downwind direction	196.81 m	269.41 m	373.96 m	445.26 m	466.23 m	575.07 m	2690.84 m	3621.81 m
Pool fire								
Distance to a radiation of 12.5 kW/m^2 (Late POOL Fire)	140.68 m	141.11 m	238.51 m	237.18 m	316.79 m	317.35 m	1641.61 m	1643.66 m
Distance to a radiation of 35.0 kW/m^2 (Late pool fire)	102.87 m	103.47 m	171.44 m	170.04 m	223.78 m	224.32 m	1149.02 m	1150.66 m
Pool Diameter (Late pool fire)	28.75 m	28.77 m	49.65 m	49.48 m	57.45 m	67.11 m	999.16 m	1000.21 m
Distance to a radiation of 12.5 kW/m^2 (Early pool fire)	120.87 m	121.40 m	209.58 m	208.28 m	288.26 m	288.52 m		
Distance to a radiation of 35.0 kW/m^2 (Early pool fire)	89.11 m	89.78 m	151.40 m	150.05 m	204.01 m	204.01 m		
Pool Diameter (Early pool fire)	24.50 m	28.05 m	43.41 m	43.24 m	52.16 m	52.23 m		
Flash fire								
Radius subjected to flash fire (safe distance)	196.81 m	269.41 m	373.96 m	445.26 m	466.23 m	575.07 m	m	m

Jet fire	Small leak		Medium leak		Large leak due to line rupture	
	Day	Night	Day	Night	Day	Night
Flame length	155.55 m	155.55 m	301.75 m	301.75 m	390.15 m	392.74 m
Distance subjected to radiation of 12.5 kW/m^2	164.88 m	164.88 m	319.89 m	319.89 m	415.03 m	417.79 m
Distance subjected to radiation of 35.0 kW/m^2	155.79 m	155.79 m	302.06 m	302.06 m	390.52 m	393.11 m

combustion temperature, experimental information and experience in practical situations (RIVM, 2009). By default, the probability of ignition for average/high reactivity must be applied for any substance, except when it has been demonstrated that its reactivity is low. Table 10 lists some substances presenting low reactivity, including Methane.

Thus, the probability of occurrence of immediate ignition as consequence of the catastrophic rupture of a 26 000 m^3 LNG tank

Table 7
Individual risk limits according to CETESB (2011).

Level	Limits
Tolerable	Individual Risk (IR) < 1×10^{-6} per year
ALARP	$1 \times 10^{-6} \le RI \le 1 \times 10^{-5}$ per year
Not tolerable	Individual Risk (IR) > 1×10^{-5} per year

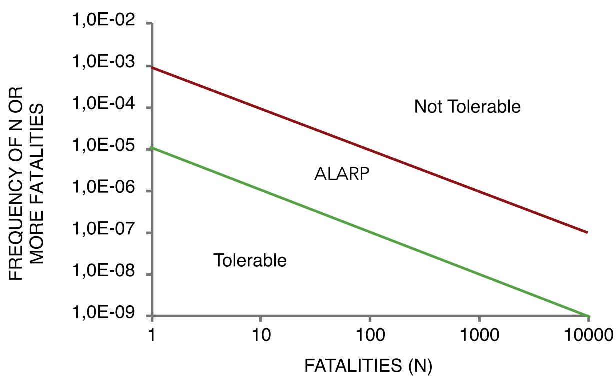

Fig. 13. FN Curve recommended by P4.621 standard as social risk criterion.

Table 10
Substances with low reactivity – Category.

Substance	CAS No 0
Methane	74-82-8
Methyl chloride	74-87-3
Ethyl chloride	75-00-3
Ammonia	7664-41-7
Methyl bromide	74-83-9
Carbon monoxide	630-08-0

instantaneous release. Moreover, the probability of no immediate ignition is obtained according to Eq. (1) as shown below.

$$P_{non-immediate\ \ ignition} = 1 - P_{immediate\ \ ignition} \tag{1}$$

In a stationary installation, an immediate ignition of instantaneous release may generate scenarios of BLEVE and a fireball, or an early pool of fire, with probability of 0.7. A delayed ignition of an unconfined vapor cloud can be assumed to be modeled as two separate events, namely, a flash fire maybe with a pool fire, depending on the scenario, and a pure explosion with a probability of 0.6 and 0.4 respectively (TNO, 2005a,b).

The value of the delayed ignition probability was assumed to be equal to 1 due to the application of the free field method. In this method, individual risk is calculated without considering the outside

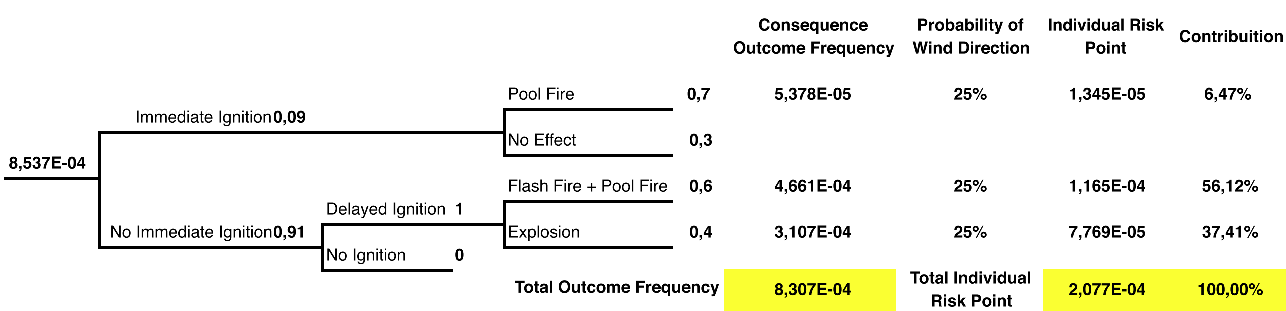

Fig. 14. Event tree for an instantaneous release of 26.000 m^3 of LNG with rainout.

Table 8
Probability of immediate ignition for stationary installations RIVM 0.

Substance category	Source term continuous	Source term instantaneous	Probability of direct ignition
Category 0	<10 kg/s	<1000 kg	0.2
average/high reactivity	10–100	1000–10 000 kg	0.5
	>100 kg/s	>10 000 kg	0.7
Category 0	<10 kg/s	<1000 kg	0.02
low reactivity	10–100 kg/s	1000–10 000 kg	0.04
	>100 kg/s	>10 000 kg	0.09
Category 1	All flow rates	All quantities	0.065
Category 2	All flow rates	All quantities	0.01
Category 3, 4	All flow rates	All quantities	0

Table 9
Classification of flammable substances (RIVM, 2009).

Category	WMS category	Limits
Category 0	Extremely flammable	Liquid substances and preparations with a flash point lower than 0 °C and a boiling point (or the start of a boiling range) less than or equal to 35 °C.
		Gaseous substances and preparations that may ignite at normal temperature and pressure when exposed to air.
Category 1	Highly flammable	Liquid substances and preparations with a flash point below 21 °C, which are not, however, extremely flammable
Category 2	Flammable	Liquid substances and preparations with a flash point greater than or equal to 21 °C and less than or equal to 55 °C
Category 3		Liquid substances and preparations with a flash point greater than 55 °C and less than or equal to 100 °C.
Category 4		Liquid substances and preparations with a flash point greater than 100 °C.

was estimated to be 0.09, and the non-immediate ignition, 0.91. The probability of immediate ignition is obtained from Table 8, considering the low reactivity of methane and the greater

population as a source of ignition. If the cloud gets outside the facility, a single ignition outcome is considered at the time when the cloud has the maximum ground level footprint area to the LFL Fraction.

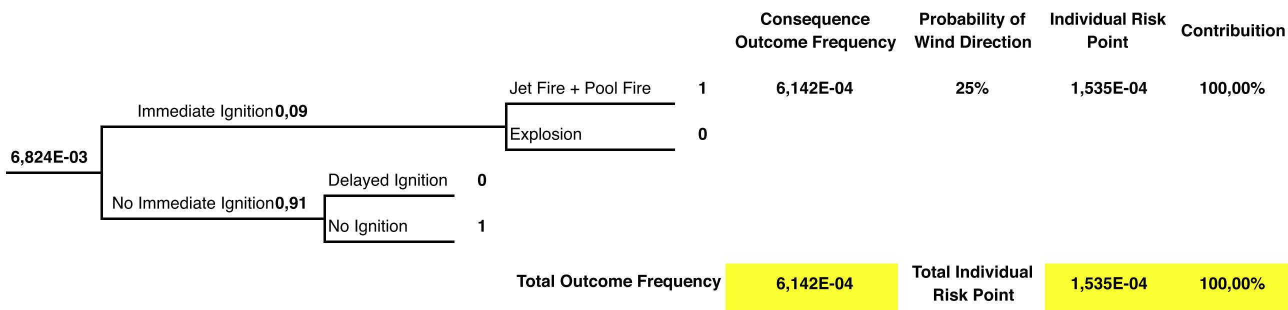

Fig. 15. Event tree for a large leak of LNG due to line rupture during the offloading operation.

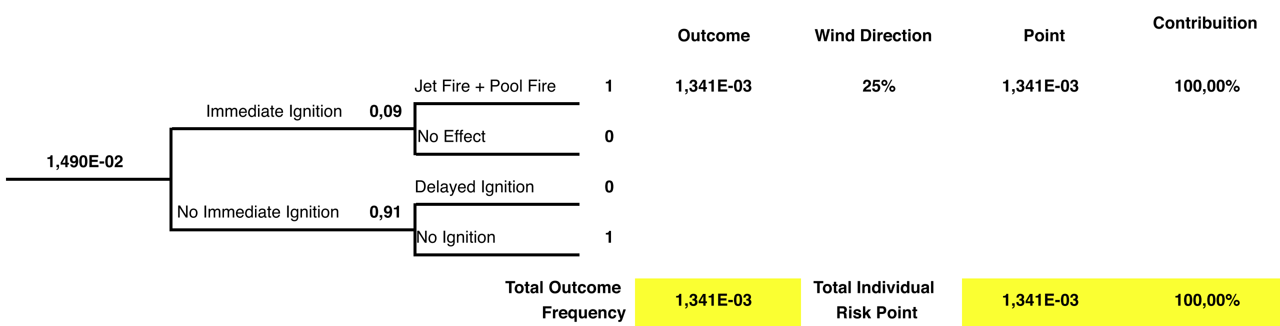

Fig. 16. Event tree for a medium leak of LNG during the offloading operation.

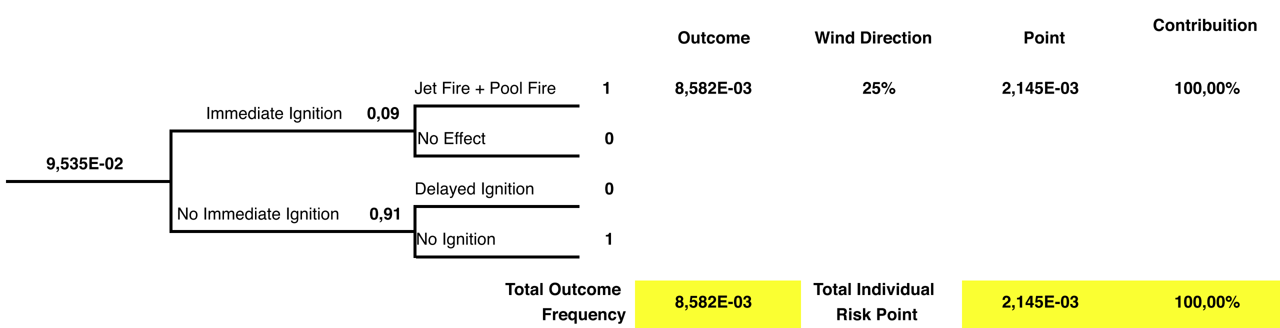

Fig. 17. Event tree for a small leak of LNG during the offloading operation.

Table 11
Population characterization.

Population category	Daytime population			Night population		
	Population	Indoors (%)	Outdoors (%)	Population	Indoors (%)	Outdoors (%)
Urban population	1000	0.93	0.07	2000	0.99	0.01
Industrial population	200			100		
University	300			150		
School	200			100		

In case of a major leak due to the line rupture, the occurrence of a single continuous release event with jet fire and pool fire is possible. This event is justified because the Free Field Method does not consider any delayed offsite ignition if the cloud has not exceeded the boundaries of installation. In this case, delayed ignition is given only if there are ignition sources onsite. Fig. 15 shows the event tree used to estimate the individual risk close to the FSRU related to the catastrophic line rupture as the initiating event during the offloading operation.

Finally, Figs. 16 and 17 show the event trees used to estimate the individual risk close to the FSRU related to medium and small leaks as the initiating event, respectively, both during the offloading operation. In both cases, the horizontal direction of the leak associated with impingement causes a residual pool fire combined with the effects of jet fire risk due to the proximity of the point. Importantly, this residual pool fire is not sufficient to cause cloud dispersion scenarios, because all the mass vaporized of LNG is burned in the pool.

4.5.2. Population characterization

The population characterization in the plant surroundings is essential to compute the social risk. Moreover, as the population is

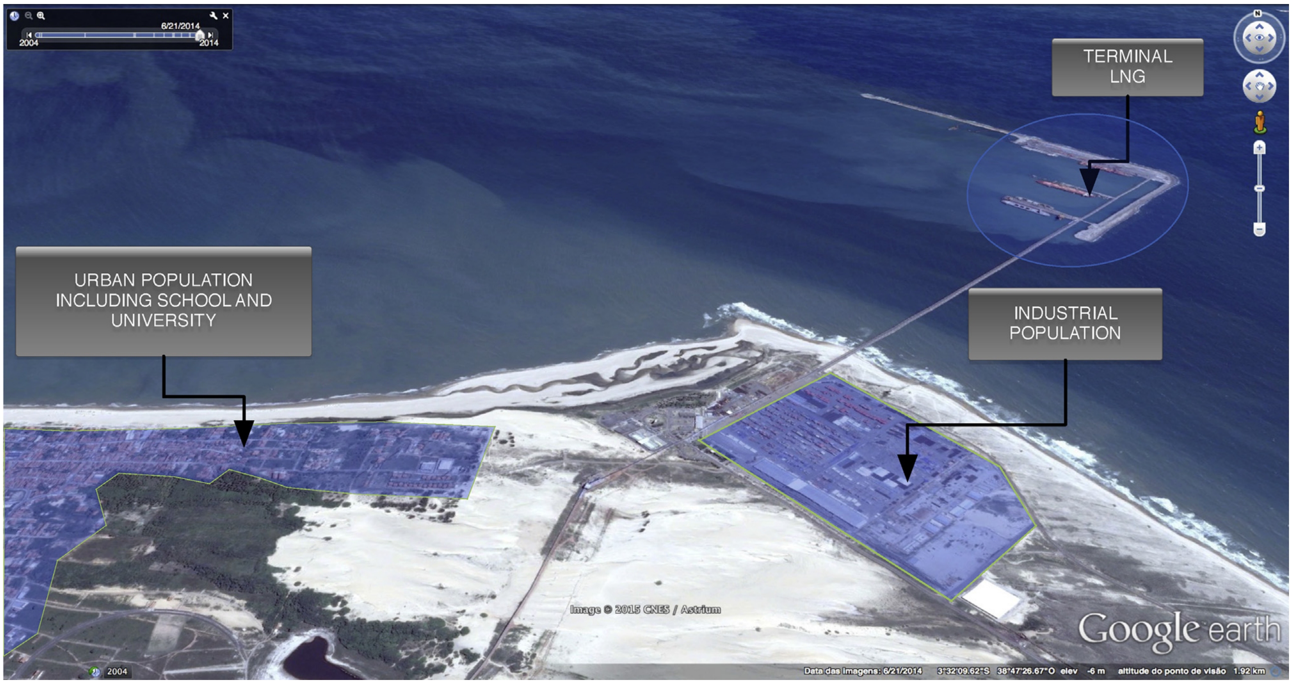

Fig. 18. Population location.

considered a source ignition, it affects both social and individual risks. Table 11 characterizes the population around the facility analyzed.

The population was considered taking into account the main urban, industrial and educational points with large concentrations of people. The population is located on the coast, distant from the

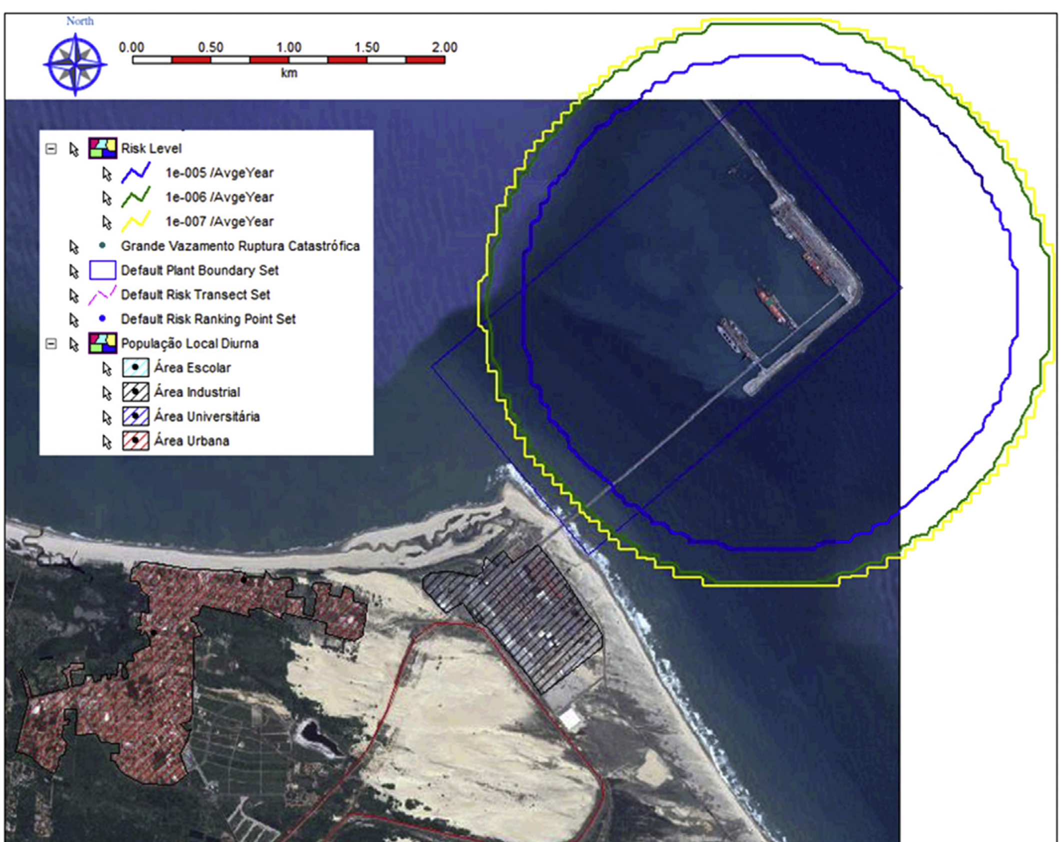

Fig. 19. Individual risk for an event of catastrophic tank rupture.

Fig. 20. 10^{-6} Individual Risk contour level for all scenarios.

Table 12
Summary of results for social and individual risk.

	Individual risk		Social risk	
	Day	Night	Day	Night
Small leak	Tolerable	Tolerable	No risk	No risk
Medium leak	Tolerable	Tolerable	No risk	No risk
Large leak (Line rupture)	Tolerable	Tolerable	No risk	No risk
Large leak (Catastrophic tank rupture)	Tolerable	Tolerable	No risk	No risk

terminal, as shown in Fig. 18.

4.6. Risk results

As the limit of 10^{-6} fatalities per year for individuals outside the plant is not exceeded, for any identified hazardous scenarios (small, medium and large leaks), the Individual Risk for the analyzed facility is tolerable.

Fig. 19 shows the representation of the individual risk for the catastrophic tank rupture event considering the same wind condition, blowing in all directions, and with the same probability of occurrence. The blue, green and yellow contours respectively represent the boundaries of individual risk for 10^{-5}, 10^{-6} and 10^{-7} fatalities/year. Although there is a possibility of the cloud

Table 13
Recommended mitigation actions.

Mitigation	Objective
Presence of exclusion zones	Prevents stranding
Presence of tugboats reservation	Prevents stranding
Presence of waterway dredging	Prevents grounding
Presence of manual and automatic emergency shutdown system	Controls leaks and fires
Connection between the terminal and the ship's system shutdown	Controls leaks and fires
Presence of relief valves on the tanks	Controls Pressure in tanks
Presence of flame arresters on tanks	Controls fires
Mooring Planner compatible with terminal	Helps lash ship with terminal
First aid in case of injuries caused by contact or ulcerations by LNG	Helps to control in an unexpected situation
Procedures for fire fighting	Helps to control in an unexpected situation
Ship evacuation procedures	Helps to control in an unexpected situation
Salvage and rescue procedures, both in case of accidents with LNG cargo or in case of collisions, groundings, extreme sea conditions, etc.	Helps to control an unexpected situation
Mooring inspection	Prevents the movement of the vessel

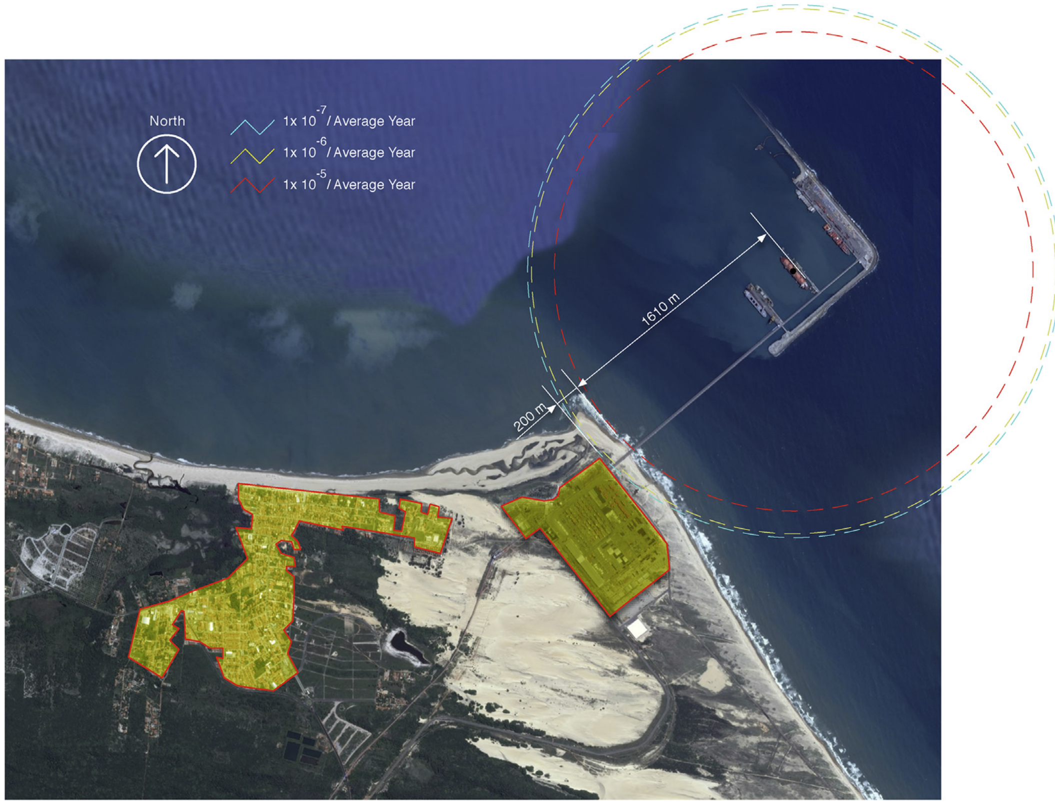

Fig. 21. Individual risk contour level for the event of catastrophic tank rupture (LNG terminal distanced 1610 m from the coast).

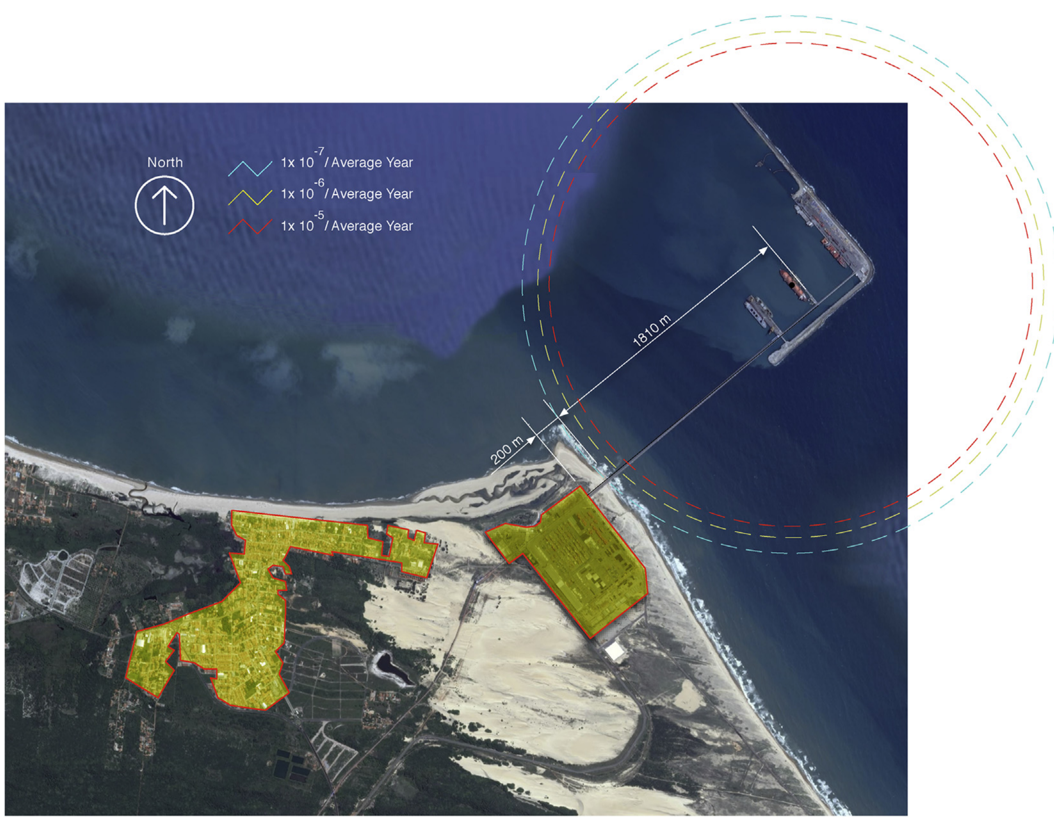

Fig. 22. Individual risk contour level for the event of catastrophic tank rupture (LNG terminal distanced 1810 m from the coast).

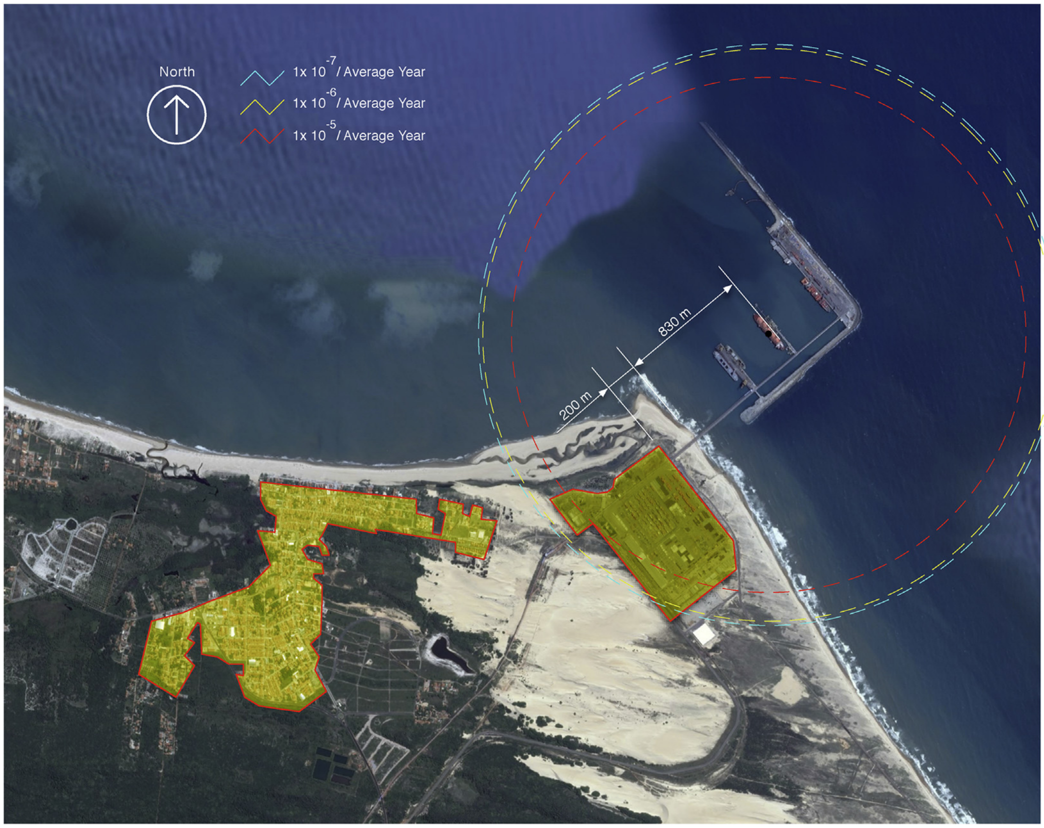

Fig. 23. Individual risk contour level for the event of catastrophic tank rupture (LNG terminal distanced 830 m from the coast).

dispersing reaching a distance of 3621.81 m from the release point in the coast direction, as seen in section 4.4, the low probability of occurrence of this event contributes to reducing the individual risk to a tolerable level.

The results for all the potential hazardous scenarios identified, at 10^{-6} risk contour level, are shown in Fig. 20.

The consequences related to the identified potential hazardous events are not enough to generate injuries or fatalities offsite boundaries. This fact is explained by the absence of a population close enough to the terminal. As the population is located away from the terminal and due to the low probability of occurrence of events, the facility analyzed presents a tolerable individual risk and no social risk. The complete risks results for all the scenarios are summarized in Table 12, which considers the simulated conditions day and night.

The propositions of mitigation and/or contingency measures

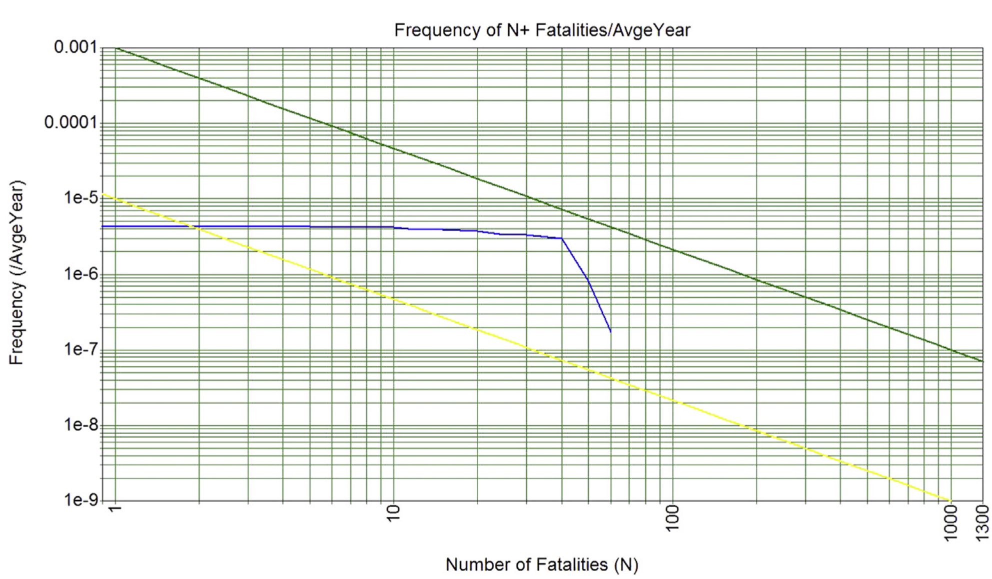

Fig. 24. Social risk curve for the event of catastrophic tank rupture (LNG terminal distanced 830 m from the coast).

are the last, but not least, step to be developed in a risk analysis. From the preliminary hazard analysis, the positive influence of each identified mitigation measure was assessed to reduce the probability of occurrence of potential hazardous events, and the influence of each contingency measure in the calculated consequences of the occurrence of possible accidents. Some devices or systems must be present on the ship or terminal and contribute to mitigating hazards. For example, the presence of exclusion zones can prevent stranding accidents. Clear safety procedures and periodic inspections are highly recommended to reduce risks. Table 13 lists some of these devices, procedures and control measures. Further information can be found in Martins and Souza (2011) where the entire mitigation actions are fully detailed.

Moreover, the fact that the 10^{-6} individual risk contour level does not reach the nearest population, i.e. Industrial population, which is 200 m away from the coast. This makes possible to approach the terminal up to about 340 m from the coast, keeping its position 1610 m away from the coast and 1810 m from the industrial population, as shown in Fig. 21. At this location, the individual risk contour level is tolerable for each individual of the current population and there is no social risk to the local population. However, if there is an urban growth, the individual risk may increase due to the increase in population near the hazardous zone.

Moving the terminal 1810 m away from the coast, as shown in Fig. 22, makes it possible to keep the individual risk on the coast at less than 10^{-6} fatalities/year and does not generate social risk to the local population, even if there is an urban growth area.

When approaching the terminal 1120 m off the coast, it is possible to see that the social risk reaches the ALARP zone and the individual risk becomes not tolerable, as shown in Figs. 23 and 24.

5. Conclusions

Despite historical analysis indicating that accidents with LNG are rare, their occurrence cannot be ignored, since there may be a chain of events that can escalate to major accidents. Some relevant events that occurred in the LNG industries were listed, including LNG offshore plants, and none of the records available led to the occurrence of significant events during transport.

Although presenting a greater possible impact area, the operation of a FSRU as an offshore terminal can present some advantages with respect to individual and social risks, compared with an onshore terminal. Moreover, the FSRU has the advantage of transporting the LNG to another location when required, which represents advantages in economic terms and contributes to the flexibility in the storage process.

Loading and unloading a LNG carrier on a FSRU terminal can lead to many undesirable scenarios, which may pose risks to the surrounding areas. However, considering a hypothetical terminal, as well as the surrounding population, along with the weather condition as described herein, both, individual and social risks can be considered tolerable according with the risk criteria proposed by the P4.621 standard (CETESB, 2011).

Considering the same risk criteria and the specified weather condition, the minimum distance from the coast of the hypothetical terminal to allow keeping the individual risk of the considered population to be less than 10^{-6} fatalities/year is of 1610 m. However, with development or population growth near the terminal, the approaching of the FSRU terminal at this distance could generate intolerable individual risks. Furthermore, considering the same weather condition, the minimum distance from the coast to the hypothetical FSRU terminal would be of 1810 m in order to keep the individual risk at any point on the coast at less than 10^{-6} fatalities/year. If the terminal is located at only 830 m off the coast, although the social risk remains outside the not tolerable risk region, it reaches the ALARP zone, and the individual risk is intolerable. In this case, the adoption of mitigation measures is essential to maintain the facility at tolerable risk levels.

Acknowledgments

This paper reports part of the overall results obtained in R&D project number 01.10.0498.00 sponsored by FINEP – Research and Projects Financing Agency, a public institution linked to the Ministry of Science and Technology in Brazil, whose support the authors gratefully wish to acknowledge. The authors also wish to acknowledge the support of the Program for Development of Human Resources (PRH19) from Petrobras and from the Brazilian National Petroleum, Natural Gas and Biofuels Agency (ANP).

Annex A. Rank of proved reserves – BP (2014).

	Late 1993	Late 2003	Late 2012	Late 2013	Share of total	R/P ratio
	Trillion cubic metres	Trillion cubic metres	Trillion cubic metres	Trillion cubic metres		
US	4.6	5.4	8.7	9.3	5.0%	3.6
Canada	2.2	1.6	2.0	2.0	1.1%	3.1
Mexico	2.0	0.4	0.4	0.3	0.2%	6.1
Total North America	8.8	7.4	11.1	11.7	6.3%	3.0
Argentina	0.5	0.6	0.3	0.3	0.2%	0.9
Bolivia	0.1	0.8	0.3	0.3	0.2%	5.2
Brazil	0.1	0.2	0.5	0.5	0.2%	1.2
Colombia	0.2	0.1	0.2	0.2	0.1%	2.8
Peru	0.3	0.2	0.4	0.4	0.2%	5.7
Trinidad & Tobago	0.2	0.5	0.4	0.4	0.2%	0.2
Venezuela	3.7	4.2	5.6	5.6	3.0%	*
Other S. & Cent. America	0.2	0.1	0.1	0.1	w	24.9
Total S. & Cent. America	5.4	6.8	7.7	7.7	4.1%	3.5
Azerbaijan	n/a	0.9	0.9	0.9	0.5%	4.3
Denmark	0.1	0.1	0.0	0.0	w	7.0

(continued on next page)

(*continued*)

	Late 1993	Late 2003	Late 2012	Late 2013	Share of total	R/P ratio
	Trillion cubic metres	Trillion cubic metres	Trillion cubic metres	Trillion cubic metres		
Germany	0.2	0.2	0.1	0.0	w	0.9
Italy	0.3	0.1	0.1	0.1	w	7.3
Kazakhstan	n/a	1.3	1.5	1.5	0.8%	2.5
Netherlands	1.7	1.4	0.9	0.9	0.5%	2.4
Norway	1.4	2.5	2.1	2.0	1.1%	8.8
Poland	0.2	0.1	0.1	0.1	0.1%	7.5
Romania	0.4	0.3	0.1	0.1	0.1%	0.6
Russian Federation	n/a	30.4	31.0	31.3	16.8%	1.7
Turkmenistan	n/a	2.3	17.5	17.5	9.4%	*
Ukraine	n/a	0.7	0.6	0.6	0.3%	3.4
United Kingdom	0.6	0.9	0.2	0.2	0.1%	0.7
Uzbekistan	n/a	1.2	1.1	1.1	0.6%	9.7
Other Europe & Eurasia	35.6	0.4	0.3	0.2	0.1%	3.4
Total Europe & Eurasia	40.5	42.7	56.5	56.6	30.5%	54.8
Bahrain	0.2	0.1	0.2	0.2	0.1%	12.1
Iran	20.7	27.6	33.6	33.8	18.2%	*
Iraq	3.1	3.2	3.6	3.6	1.9%	*
Kuwait	1.5	1.6	1.8	1.8	1.0%	*
Oman	0.2	1.0	0.9	0.9	0.5%	30.7
Qatar	7.1	25.3	9	24.7	13.3%	*
Saudi Arabia	5.2	6.8	8.2	8.2	4.4%	9.9
Syria	0.2	0.3	0.3	0.3	0.2%	3.9
United Arab Emirates	5.8	6.0	6.1	6.1	3.3%	*
Yemen	0.4	0.5	0.5	0.5	0.3%	46.3
Other Middle East	0.0	0.1	0.2	0.2	0.1%	35.3
Total Middle East	44.4	72.4	3	80.3	43.2%	*
Algeria	3.7	4.5	4.5	4.5	2.4%	57.3
Egypt	0.6	1.7	2.0	1.8	1.0%	32.9
Libya	1.3	1.5	1.5	1.5	0.8%	*
Nigeria	3.7	5.1	5.1	5.1	2.7%	*
Other Africa	0.7	1.0	1.2	1.2	0.7%	6.9
Total Africa	10.0	13.9	14.4	14.2	7.6%	69.5
Australia	1.0	2.4	3.8	3.7	2.0%	85.8
Bangladesh	0.3	0.4	0.3	0.3	0.1%	12.6
Brunei	0.4	0.3	0.3	0.3	0.2%	23.6
China	1.7	1.3	3.3	3.3	1.8%	28.0
India	0.7	0.9	1.3	1.4	0.7%	40.2
Indonesia	1.8	2.6	2.9	2.9	1.6%	41.6
Malaysia	1.8	2.5	1.1	1.1	0.6%	15.8
Myanmar	0.3	0.4	0.3	0.3	0.2%	21.6
Pakistan	0.7	0.8	0.6	0.6	0.3%	16.7
Papua New Guinea	^	^	0.2	0.2	0.1%	*
Thailand	0.2	0.4	0.3	0.3	0.2%	6.8
Vietnam	0.1	0.2	0.6	0.6	0.3%	3.3
Other Asia Pacific	0.3	0.5	0.3	0.3	0.2%	7.5
Total Asia Pacific	**9.3**	**12.7**	**15.2**	**15.2**	**8.2%**	**1.1**
Total World	**118.4**	**155.7**	**185.3**	**185.7**	**100.0%**	**5.1**
Of which: OECD	14.6	15.3	18.7	19.2	10.3%	6.0
Non-OECD	103.8	140.4	166.6	166.5	89.7%	6.7
European Union	3.7	3.2	1.6	1.6	0.8%	0.7
Former Soviet Union	35.3	36.9	52.8	52.9	28.5%	8.2

*: less than 0.05.
w: Less than 0.05%.
Notes: Proved reserves of oil – Generally taken to be those quantities that geological and engineering information indicate with reasonable certainty can be recovered in the future from known reservoirs under existing economic and operating conditions.
Reserves-to-production (R/P) ratio – If the reserves remaining at the end of any year are divided by the production in that year, the result is the length of time that those remaining reserves would last if production were to continue at that rate.
Source of data – The estimates in this table have been compiled using a combination of primary official sources and third-party data from Cedigaz and the OPEC Secretariat. BP (2013).

Annex B. Some accidents in the LNG industry.

Date	Location	Description	Fatalities	Cost (US$ millions)
October 20th, 1944	Cleveland, Ohio, USA	At the peak-shaving plant, a leak in a tank spreads LNG into the street and storm sewer system, resulting in an explosion and fire. The main cause was the tank built with a steel alloy that had low-nickel content, which made the alloy brittle when exposed to the extreme cold of LNG.	130	890
May 3, 1965	Canvey Island UK	An explosion occurred during the work of the LNG transport onshore.	1	2
March 18th, 1971	La Spezia, Italy	This accident was caused by "rollover" which is a sudden increase in pressure resulting in the release of large amounts of vapor. In this case, about 2000 tons of LNG vapor discharged from the tank safety valves and vents over a period of a few hours, damaging the roof of the tank.	0	1
February 10th, 1973	Staten Island, New York, USA	After a power failure and the automatic closure of the main liquid line valves, 40 gallons of LNG leaked as it was being loaded onto a barge. The LNG leaked from a one-inch nitrogen-purge globe valve on the vessel liquid header, causing several fractures on the deck plate	40	15
April 18th, 1997	Arzew, Algeria	LNG release at the facility, causing fire and explosion. The cause was a failure in a valve whose material was aluminum. This valve failed when it came into contact with the cryogenic fluid.	1	1
October 6th, 1979	Cove Point, Maryland, USA	An explosion occurred inside the electrical substation at the receiving end of Cove Point. The LNG leaked through the electric pump seal. The vaporized natural gas went through 70 m of pipes and electrical cables penetrating the substation. At the time of construction, no gas detectors were installed in the building, because it was not expected to have natural gas in this area.	1	9
December 20th, 1983	Bontang, Indonesia	A rupture in an LNG plant occurred as a result of over-pressurization of the heat exchanger caused by a closed valve on a blow-down line. The exchanger failed and the explosion occurred.	0	15
May 10th, 1988	Boston, Massachusetts, USA	LNG facility spilled 30 000 gallons.	0	12
January 19th, 2004	Skikda, Algeria	A steam boiler that was part of an LNG production plant exploded and caused a vapor-cloud explosion and fire. The explosions and fire destroyed a portion of the LNG plant and caused 27 deaths, 74 injuries, and financial loss outside the plant boundaries.	27	54

Annex C. Some accidents involving LNG tankers.

Year	Ship name	Type of cargo containment	Injuries/Fatalities	LNG spill	Incident category	Incident description
1969	Polar Alaska (Methane Polar)	Membrane	No	Yes	CCS	Violent sloshing of LNG in refrigerated tank en route to Alaska caused cable tray to break loose. This, in turn, slashed the thin membrane cargo tank wall releasing contents. No fire or explosion reported. Sloshing of the LNG heel in No. 1 tank caused part of the supports for the cargo pump electric cable tray to break loose, resulting in several perforations of the primary barrier (invar membrane). LNG leaked into the interbarrier space. No LNG released from the secondary
1970	Arctic Tokyo	Membrane	No	No	CCS	A few hours out of Japan, heavy seas caused sloshing of cargo tanks in LNG ship steaming from Japan to Alaska. A thin membrane wall bent in four places and a half inch crack formed in a weld seam. Sloshing of the LNG heel in No. 1 tank during bad weather caused local deformation of the primary barrier (invar membrane) and supporting insulation boxes. LNG leaked into the interbarrier space at one location. No LNG released from the secondary barrier.
1978	Khannur	Spherical	No	No	Col	Collision with cargo ship Hong Hwa in the Straits of Singapore. Minor damage. No LNG released
1979	El Paso Paul Kayser	Membrane	No	No	Grd	Stranded. Severe damage to bottom, ballast tanks, motors water damaged, bottom of containment system set up. Stranded in the straits of Gibraltar. Was subsequently re-floated and towed to harbor to discharge cargo. Vessel was dry-docked when survey revealed extensive damage.
1979	Isabella	Membrane	No	No	FE	Explosion in engine room.
1979	LNG Capricorn	Spherical	No	–	CCS	Cargo compressor explosion while on voyage.
1980	LNG Libra	Spherical	No	No	EM	Shaft moved against rudder. Tail shaft fractured. Propeller tail shaft fractured while enroute from Indonesia to Japan, leaving the ship without propulsion. Ship towed to the Philippines; cargo transferred to sister ship LNG Leo, then towed to Singapore for repairs.

(continued on next page)

(*continued*)

Year	Ship name	Type of cargo containment	Injuries/Fatalities	LNG spill	Incident category	Incident description
1980	Arctic Tokyo	Membrane	No	–	CCS	Tank damage whilst on voyage between Nikiski and Yokohama.
1980	LNG Libra	Spherical	No	No	EM	Forward pumproom flooded at sea due to defects in emergency fire pump motor and forward transfer pump motor.
1981	LNG Capricorn	Spherical	No	No	EM	Turbo generator damage. Sustained vibration and journal bearing damages.
1981	LNG Virgo	Spherical	No	No	EM	Boiler damage whilst on voyage.
1981	LNG Libra	Spherical	No		HW	Damage to weather deck and rudder in way of cargo domes whilst on voyage from Tobata to Botang in heavy weather. Various weather deck and stiffening fractures in way of all 5 cargo tank domes.
1982	Descartes	Membrane	No	No	EM	Lost rudder at sea. Towed to port.
1982	Tenaga Satu	Membrane	No	No	EM	Machinery damage whilst on voyage from Dunkirk to Marseilles. Malfunction of cargo and stripping pumps during gas trials. Nitrogen line in No 1 tank has sustained damage.
1982	LNG Gemini	Spherical	No	No	Cnt	Struck submerged object whilst on voyage from Arun terminal to Osaka. On a blade slightly bent at the tip.
1984	LNG Gemini	Spherical	No	–	HW	Sustained heavy weather damage whilst on voyage from Osaka to Botang. Ballast tank damage. Ballast tank found cracked in way of weld.
1986	LNG Virgo	Spherical	No	No	Col	Slightly damaged by collision with MFV Koshin Maru.
1987	Pollenger (LNG Challenger)	Spherical	No	No	EM	Sustained main condenser circulating pump failure whilst on voyage from New York to Sakaido.
1990	Bachir Chihani	Membrane	No	No	CCS	Sustained structural cracks allegedly caused by stressing and fatigue in inner hull. Cracks in the inner hull allowed ballast water into the space behind the cargo hold insulation
1990	Louisiana (LNG Abuja)	Spherical	No	No	EM	Sustained No 1 turbo-generator damage in the Gibraltar area.
1997	Northwest Swift	Spherical	No	No	Col	Collision with fishing vessel. Damage to port side and bulwark. No water ingress. Collided with fishing vessel about 400 km from Japan. Some damage to hull, but no ingress of water and no loss of LNG.
1998	LNG Bonny	Membrane	No	No	EM	Had complete power failure and drifted 90 miles off Miyakoshima. Tug on scene, repair crew aboard vessel, repairs completed and resumed voyage. Electric power failure while enroute from Indonesia to Korea. Salvors repaired generator.
2000	Hanjin Pyeong Taek	Membrane	No	No	Col	Collision with bulk carrier Corali near Busan. Damage occurred to shell plating.
2001	Methane Polar	Membrane	No*	No	Col	Collision with bulker. Minor hull damage. In collision with bulk carrier Eastwind off Algeria. Sustained holing to bow. Subsequently arrived in Piraeus for repairs.
2003	Century	Spherical	No	No	EM	Sustained main engine damage offshore Algeria. Under tow by two tugs to Syros Shipyards.
2003	Hoegh Galleon (Pollenger)	Spherical	No	No	EM	Gearbox problems. Being towed to Ferrol. Major repairs.
2004	British Trader	Membrane	No	No	FE	Minor electrical fire onboard, damaged one transformer, contained and underway
2004	Tenaga Lima	Membrane	No	No	Cnt	Made contact with a submerged rock due to a strong southerly current. The starboard side shell plating in way of No 1 membrane tank was reportedly heavily damaged but did not require temporary repairs at Mokpo. Sailed to Yokohama for permanent repairs.

CCS = Cargo Containment System; Col = Collision; Grd = Grounding; EM = Equipment or Machinery HW= Heavy Weather; Cnt = Contact; FE=Fire or Explosion.
Note: * 3 injuries and one fatality of bulk carrier crew.

Annex D. LNG loading system – input data.

Area	Segment	Equipment	Base element				
			Type	Number (*)	Size (in)	Pressure (atm)	Liquid (vol) (%)
Connection System	Manifold (Port-Side)	Open/Close Valves	VALVE_MAN	6	12	7757	100
		Containment Valve	VALVE_MAN	6	12	7757	100
		Containment Valve	VALVE_MAN	1	12	7757	100
		Pipeline	PIPE_PROC	20	12	7757	100
	Manifold (Starboard-Side)	Containment Valve	VALVE_MAN	4	12	7757	100
		Containment Valve	VALVE_MAN	2	12	7757	100
		Pipeline	PIPE_PROC	10	12	7757	100
Delivery System	Pipeline	Main Pipeline	PIPE_PROC	328	12	7757	100
		Secondary Pipeline	PIPE_PROC	32	12	7757	100
		Secondary Pipeline	PIPE_PROC	10	12	7757	100
	Valves	Containment Valve	VALVE_MAN	2	12	7757	100
		Containment Valve	VALVE_MAN	1	12	7757	100
Storage System	Valves (Storage Tank 1)	Open/Close Valves	VALVE_MAN	2	12	7757	100
		Containment Valve	VALVE_MAN	1	12	7757	100
		Secondary Pipeline	VALVE_MAN	3	12	7757	100
	Valves (Storage Tank 2)	Open/Close Valves	VALVE_MAN	2	12	7757	100

(*continued*)

Area	Segment	Equipment	Base element				
			Type	Number [(*)]	Size (in)	Pressure (atm)	Liquid (vol) (%)
		Containment Valve	VALVE_MAN	1	12	7757	100
		Containment Valve	VALVE_MAN	3	12	7757	100
	Valves (Storage Tank 3)	Open/Close Valves	VALVE_MAN	2	12	7757	100
		Containment Valve	VALVE_MAN	1	12	7757	100
		Containment Valve	VALVE_MAN	3	12	7757	100
	Valves (Storage Tank 4)	Open/Close Valves	VALVE_MAN	2	12	7757	100
		Containment Valve	VALVE_MAN	1	12	7757	100
		Containment Valve	VALVE_MAN	3	12	7757	100
	Valves (Storage Tank 5)	Open/Close Valves	VALVE_MAN	2	12	7757	100
		Containment Valve	VALVE_MAN	1	12	7757	100
		Containment Valve	VALVE_MAN	3	12	7757	100
	Storage Tank	Storage Tanks	VESSEL_STO_ATM	5	12	7757	100
Relief System	Relief Valve (Port-Side)		VALVE_ACT_NON_P/L	6	12	7747	100
	Relief Valve (Starboard-Side)		VALVE_ACT_NON_P/L	6	12	7747	100
	Relief Valve (Main Pipeline)		VALVE_ACT_NON_P/L	8	12	7747	100
	Tank 1 Inlet Relief Valve		VALVE_ACT_NON_P/L	4	12	7747	100
	Tank 2 Inlet Relief Valve		VALVE_ACT_NON_P/L	4	12	7747	100
	Tank 3 Inlet Relief Valve		VALVE_ACT_NON_P/L	4	12	7747	100
	Tank 4 Inlet Relief Valve		VALVE_ACT_NON_P/L	4	12	7747	100
	Tank 5 Inlet Relief Valve		VALVE_ACT_NON_P/L	4	12	7747	100
	Pipeline		PIPE_PROC	14	12	7747	100

[(*)] Note: The column Number refer to number of elements or lenght of pipeline (m).

Annex E. LNG unloading system – input data.

System	Equipment		Base element				
			Type	Number	Size (in)	Pressure (atm)	Liquid (vol) (%)
Storage System	Valves (Storage Tank 1)		VALVE_ACT_NON_P/L	2	12	7757	100
			VALVE_MAN	5	12	7757	100
			VALVE_MAN	1	12	7757	100
	Valves (Storage Tank 2)		VALVE_ACT_NON_P/L	2	12	7757	100
			VALVE_MAN	3	12	7757	100
			VALVE_MAN	1	12	7757	100
	Valves (Storage Tank 3)		VALVE_ACT_NON_P/L	2	12	7757	100
			VALVE_MAN	3	12	7757	100
			VALVE_MAN	1	12	7757	100
	Valves (Storage Tank 4)		VALVE_ACT_NON_P/L	2	12	7757	100
			VALVE_MAN	3	12	7757	100
			VALVE_MAN	1	12	7757	100
	Valves (Storage Tank 5)		VALVE_ACT_NON_P/L	2	12	7757	100
			VALVE_MAN	3	12	7757	100
			VALVE_MAN	1	12	7757	100
	Storage Tanks		VESSEL_STOR_ATM	5	12	7757	100
Delivery System	Main Pipeline		PIPE_PROC	328	12	7757	100
	Secondary Pipeline	Pipeline Storage – Main Pipeline	PIPE_PROC	10	12	7757	100
		Main Pipeline – Manifold	PIPE_PROC	32	12	7757	100
	Containment Valve		VALVE_MAN	2	12	7757	100
	Containment Valve		VALVE_MAN	1	12	7757	100
Connection System	Manifold (Port-Side)	Open/Close Valve	VALVE_MAN	6	12	7757	100
		Containment Valve	VALVE_MAN	1	12	7757	100
		Containment Valve	VALVE_MAN	6	12	7757	100
		Pipeline	PIPE_PROC	20	12	7757	100
	Manifold (Starboard-Side)	Containment Valve	VALVE_MAN	4	12	7757	100
		Containment Valve	VLVE_MAN	2	12	7757	100
		Pipeline	PIPE_PROC	10	12	7757	100
Relief System	Relief Valve (Port-Side)		VALVE_ACT_NON_P/L	6	12	7757	100
	Relief Valve (Starboard-Side)		VALVE_ACT_NON_P/L	6	12	7757	100
	Relief Valve (Main Pipeline)		VALVE_ACT_NON_P/L	6	12	7757	100
	Tank 1 Inlet Relief Valve		VALVE_ACT_NON_P/L	4	12	7757	100
	Tank 2 Inlet Relief Valve		VALVE_ACT_NON_P/L	4	12	7757	100
	Tank 3 Inlet Relief Valve		VALVE_ACT_NON_P/L	4	12	7757	100
	Tank 4 Inlet Relief Valve		VALVE_ACT_NON_P/L	4	12	7757	100
	Tank 5 Inlet Relief Valve		VALVE_ACT_NON_P/L	4	12	7757	100
	Pipeline		PIPE_PROC	13	12	7757	100

[(*)] Note: The column Number refer to number of elements or lengtht of pipeline.

Annex F. Models for analyzing consequences.

Model	Simulated event	Description
GASP Model – Gas Accumulation over Spreading Pools (TNO, 2005a,b; Witlox, 2006)	Pool formation, dispersion and evaporation	The goal of the model is the description of the dispersion and the evaporation of the pool in order to estimate the evaporation rate and the size of the pool. Applicable to pools formed on soil or water, by any liquid, regardless of its boiling point, the model takes into account both mass transfer due to environmental conditions and due to heat transfer to the environment. Dispersion pools formed by instantaneous or time-dependent leakages can be modeled using GASP with the option of using physical constraints to the dispersion (Pools (TNO, 2005a,b; Witlox, 2006; Webber, 1990).
PVAP Model Pool Vaporization (TNO, 2005a,b; CAS, 2015)	Pool formation, dispersion and evaporation.	The PVAP model simulates the formation and dispersion of the pool released on soil or over water and provides the flow of the steam deriving from it. It uses different sub-models be the pool formed on water or soil and the vaporization rates are taken into account while the pool is spreading. For the dispersion of the pool on the ground, the model considers the influence of the heat conducted by the soil, the convection of the air, radiation and the vapor diffusion to evaluate the vaporization rates. If the pool is spreading on water, the model also considers the dissolution of the material in the water and, if the liquid released is ammonia, the chemical reaction is taken into account, too. In all the cases, this model is fully capable of simulating the dispersion of the pool, no matter the boiling temperature of the liquid. Initially, the temperature of the pool is assumed to be the same as the released liquid and, at each time step, the values of the vaporization rate, the size of the pool and its temperature are evaluated. This model also considers the formation of the pool as being concentric to the rainout point and it is also capable of simulating the dispersion of the pool as a result of a continuous, instantaneous, finite duration or variable flow release, until it finds a containment barrier or reaches the minimum thickness. If the pool finds a barrier, its radius is limited to the containment radius (TNO, 2005a,b; CAS, 2015).
Unified Dispersion Model – UDM (Harper, 2009)	Cloud Dispersion	UDM is a model that uses integral calculations to simulate the dispersion of the cloud resulting from instantaneous, continuous or finite duration releases, no matter if the release is constant or time-varying, at the height of the ground or higher, with or without the occurrence of jets in any direction. When the cloud is consisted of two phases – liquid and vapor -, this model is capable of taking into account the vaporization of the liquid portion of the cloud before it reaches the ground, incorporating the vaporized portion into the generated cloud. For modeling the formation of pool, spreading and its vaporization, UDM incorporates the PVAP model and, in doing so, the steam generated in the pool is added to the dispersion cloud which thus receives a variable flow of steam within time. The possibility of variation in wind speed, pressure and temperature as a function of releases that are not in the ground is another difference of this model when compared to others. Depending on the kind of equations, UDM also simulates the transition from dense cloud to passive cloud, which means it is no longer necessary to couple different models for analyzing different stages of dispersion (Harper, 2009).
Gaussian Plume Model (TNO, 2005a,b)	Passive cloud dispersion	The Gaussian model is applied to passive cloud dispersion on flat ground and uniform and on stationary atmospheric condition. This model does not consider changes commonly noticed in environmental condition during the day and it is not recommended in cases with cloud dispersion for periods above three hours (TNO, 2005a,b).
SLAB Model (Ermak, 1990)	Dispersion Model for denser – than- air – releases	The SLAB model treats denser-than-air releases by solving the one-dimensional equations of momentum, conservation of mass, species, and energy, and the equation of state. SLAB handles release scenarios including ground level and elevated jets, liquid pool evaporation, and instantaneous volume sources (Ermak, 1990).
Chamberlain Model (TNO, 2005a,b; Chamberlain, 1987)	Thermal radiation emitted by jet fire	Semi-empirical model that considers a flame with a solid body (conical frustum) emitting radiation from its surface. This model is validated with experiments in wind tunnel testing and in true scale. This model is limited to jets in the vertical or with an inclination angle lower than 45° to the vertical and consisting only of steam (TNO, 2005a,b; Chamberlain, 1987).

(*continued*)

Model	Simulated event	Description
JFSH-Cook Model (Oke, 2005; TNO, 2005a,b; Cook et al., 1990)	Thermal radiation emitted by jet fire	Based on the model proposed by Cook et al. (1990), allows analyzing the fire resulting jet of release liquid or multi-phase product (liquid + vapor) (Oke, 2005; TNO, 2005a,b; Cook et al., 1990).
JFSH-Johnson Model (Johnson et al., 1994; Oke, 2005; TNO, 2005a,b)	Thermal radiation emitted by jet fire	An improvement of the model proposed by Chamberlain (1987), allows analyzing horizontal jets or angle of inclination greater than 45° from the vertical (Johnson et al., 1994; Oke, 2005; TNO, 2005a,b).
API RP527 (API, 1969; Baron, 1954; Cook et al., 1990)	Thermal radiation emitted by jet fire	Treats the flame as a banana shaped plume. This model does not model angled jets, working only with angle jet to downwind, horizontal or upwards (API, 1969; Baron, 1954; Cook et al., 1990).

References

ANP – Agência Nacional de Petróleo, 2007. Gás Natural e Biocombustíveis. Despacho do Superintendente No1.011/2007 – DOU 16.10.2007.

ANP – Agência Nacional do Petróleo, 2010. Gás Natural e Biocombustíveis. O Gás Natural Liquefeito no Brasil, Rio de Janeiro.

API – American Petroleum Institute, 1969. Guide to Pressure Relief and Depressuring Systems, p. 53. API RP521 Par 5.3.

Baron, T., 1954. Reactions in turbulent free jets – the turbulent diffusion flame. Chem. Eng. Prog.

Blakwell, B., Skaar, H., 2009. Delivering the World's first FSRUs. In: 24th World Gas Conference. Buenos Aires.

BP-British Petroleum, 2014. BP Statistical Review of World Energy 2014.

CCNR – Central Commission for the navigation of the Rhine, 2010. International Safety Guide for Inland Navigation Tank Barg and Terminals – ISGINTT, first ed. Oil Companies International Marine Forum.

CETESB – Environmental Company of São Paulo State, 2011. CETESB P4.261- Risk of Accident of Technological Origin – Method for Decision Making and Reference Terms.

CH IV, 2015. Safety History of International LNG Operations. Available at: http://www.ch-iv.com/ (access on 19.09.15.).

Chamberlain, G.A., 1987. Developments in design methods for predicting thermal radiation from flares. Chem. Eng. Res. Des. 65, 299–309.

CAS – Chemical Abstracts Service available at http://www.cas.org, access on 02.09.15, 2015.

Cook, J., Woodward, J.L., 1993. A new integrated model for pool spreading, evaporation, and solution on land and in water. In: International Conference on Safety, Health and LP in the Oil, Chemical and Process Industries. Singapore. Feb, pp. 15–19.

Cook, J., Bahrami, Z., Whitehouse, R.J., 1990. A comprehensive program for calculation of flame radiation levels. J. Loss Prev. 3, 150–155.

Ditali, S., Fiore, R., 2007. A Realistic Assessment of LNG Hazard and Consequences of Release scenarios.Health, Safety & Environment – Design. Snamprogetti SpA Viale de Gasperi, Italy.

DNV – Det Norske Veritas, 2013. DNV Failure Frequency Guidance (Norway).

DNV – Det Norske Veritas, 2009a. PHAST RISK Software. Version 6.7.

DNV – Det Norske Veritas, 2009b. Leak Software. Version 3.3.

EHSNR, 2015. Online Notification and Registration of Environmentally Hazardous Substances. Available at: https://www.e-ehs.doe.gov.my/app/webroot/portal/ (access on 03.08.15.).

Ermak, D.L., 1990. User's Manual for Slab: an Atmospheric Dispersion Model for Denser-than-air Releases.

Eyres, D.J., Bruce, G.J., 2012. Ship Construction, Butterworth-heinemann, seventh ed. Elsevier.

Flemish Government, 2009. Handbook Failure Frequencies 2009 for Drawing up a Safety Report. LNE Department. Environment, Nature and Energy Policy Unit. Safety Reporting Division.

GexCon, A.S., 2013. FLACS Software: Version 10.4.

Harper, H., 2009. UDM Theory Document (DNV Report).

HSE – Health and Safety Executive, 2015. Hydrocarbon Release Reporting and Statistics available at: http://www.hse.gov.uk/offshore/hydrocarbon.htm (access on 03.08.15.).

IMO—International Maritime Organization, 2007. FSA – Liquefied Natural Gas (LNG) Carries – Details of the Formal Safety Assessment. International Maritime Organization, London.

IMO—International Maritime Organization, 2013. Revised Guidelines for Formal Safety Assessment (FSA) for Use in the IMO Rule-making Process. International Maritime Organization, London.

Jang, C.B., Choi, S.W., Baek, J.B., 2015. CFD modeling and fire damage analysis of jet fire on hydrogen pipeline in a pipe rack structure. Int. J. Hydrogen Energy 40 (45), 15760–15772. http://dx.doi.org/10.1016/j.ijhydene.2015.09.070.

Johnson, A.D., Brightwell, H.M., Carsley, A.J., 1994. A model for predicting the thermal radiation hazard from large scale horizontally released natural gas jet fires. Trans. IChemE 72 (Part B), 157–166.

Martins, M.R., Schleder, A.M., 2012. Reliability analysis of the regasification system on board of a FSRU using Bayesian networks. In: Gupta, S.B. (Ed.), Natural Gas: Extraction to End Use, first ed. Pennsylvania, USA: INTECH Open Science, pp. 143–158.

Martins, M.R., Pestana, M.A., Primon, R.B., Natacci, F.B., 2014. Risk analysis of undesirable events during transport, loading and unloading of Liquefied Natural Gas (LNG) on ships. In: International Conference on Maritime Technology and Engineering – MARTECH2014, Lisbon. Proceedings of 2nd International Conference on Maritime Technology and Engineering – MARTECH2014, pp. 1–7.

Martins, M.R., Souza, G.F.M., 2011. Levantamento e detalhamento dos eventos indesejáveis a serem considerados. Technical report number 3. FINEP, São Paulo.

Martins, M.R., Souza, G.F.M., 2013. Levantamento e detalhamento dos eventos indesejáveis a serem considerados. Technical report number 7. FINEP, São Paulo.

Martins, M.R., Souza, G.F.M., Ikeda, N.H., 2011. Consequence analysis of a liquefied floating production storage offloading (LNG FPSO) leakage. In: Proceedings of the ASME 2011 30th International Conference on Ocean. Offshore and Arctic Engineering, Rotterdam, The Netherlands.

Moonis, M., Wilday, A.J., Wardman, M.J., 2010. Semi-quantitative risk assessment of commercial scale supply chain of hydrogen fuel and implications for industry and society. Process Saf. Environ. Prot. 88 (2), 97–108.

Natacci, F.B., Martins, M.R., Ikeda, N.H., 2010. Consequence analysis of a liquefied natural gas leakage. In: Proceedings of the ASME 2010 29th International Conference on Ocean. Offshore and Arctic Engineering, Shangai, China.

Oke, A.O., 2005. JSFH (Jet Fire) Theory Document (DNV Report).

OTA – Office of Technology Assessment, 1977. In: Proceedings of the OTA Congress of the United States – Transportation of Liquefied Natural Gas, September, 1977. Washington, DC.

Petrobras, 2015. Image available at http://exposicao60anos.agenciapetrobras.com.br/imagens/home-momentos/2000/momento47/fotos-relacionadas-alta/terminal-de-gnl-de-pecem2-creditos-agencia-petrobras2.jpg, access on 03.08.15.

Pitblado, R., Baik, J., Raghunathan, V., 2006. LNG decision making approaches compared. J. Hazard. Mater. 130 (1–2), 148–154. http://dx.doi.org/10.1016/j.jhazmat.2005.07.081. PubMed PMID: WOS:000236437700021.

Ramos, M.A., Droguett, E.L., Martins, M.R., Souza, H.P., 2011. Quantitative risk analysis and comparison for onshore and offshore LNG terminals: the Port of Suape—Brazil case. In: Proceedings of the ASME 2011 30th International Conference on Ocean. Offshore and Arctic Engineering, Rotterdam, Netherlands.

Ramos, M.A., Droguett, E.L., Martins, M.R., Souza, H.P., 2014. Comparison of possible consequences of LNG leakages in offshore and onshore terminals: the case of the Port of Suape in the northeastern Brazil. Int. J. Model. Simul. Pet. Ind. 8 (1).

RIVM, 2009. Reference Manual BEVI Risk Assessments. v3.1, Jan 1st 2009. Centre for External Safety, Netherlands National Institute of Public Health and the Environment.

Schleder, A.M., Martins, M.R., Souza, G.F.M., 2011a. Preliminary risk analysis of a liquefied natural gas regasification system in an offshore unit. In: Proceedings of the International Conference on Vulnerability and Risk Analysis and Management, College Park, MD. http://dx.doi.org/10.1061/41170(400)48.

Schleder, A.M., Martins, M.R., Souza, G.F.M., 2011b. Bayesian networks on risk analysis of a regasification system on an offshore unit. In: International Conference on Ocean, Offshore and Arctic Engineering, 2011, Rotterdam, Netherlands. Proceedings of the ASME 2011 30th International Conference on Ocean. Offshore and Arctic Engineering, pp. 1–8.

Schleder, A.M., Martins, M.R., 2013. Comparative evaluation of the cloud dispersion of a liquefied natural gas leakage using the UDM and a CFD model. In: International Conference on Ocean, Offshore and Arctic Engineering, 2013, Nantes. Proceedings of the ASME 2013 32th International Conference on Ocean. Offshore and Arctic Engineering – OMAE, pp. 1–8.

Sovacool, B.K., 2008. The costs of failure: a preliminary assessment of major energy accidents, 1907 – 2007. Energy Policy 36, 1802–1829.

TNO – The Netherlands Organization of Applied Scientific Research, 2005a. Methods for the Calculation of Physical Effects – Due to Releases of Hazardous Materials (Liquids and Gases) – Yellow Book, third ed. Committee for the Prevention of Disasters. Second revised print, 2005.

TNO – The Netherlands Organization of Applied Scientific Research, 2005b. Guidelines for Quantitative Risk Analysis (Purple Book). In: Publication Series on Dangerous Substances 3. Ministry of VROM, p. 2005.

Webber, D.M., 1990. Model for Pool Spreading and Vaporization and its Implementation in the Computer Code GASP. SRD/HSE-report R507.

Witlox, H., 2006. PVAP Theory Document (DNV Report).

Woodward, J.L., Pitblado, R., 2010. LNG Risk Based Safety: Modeling and Consequence Analysis.